BENZOPHENONE PHOTOPROBES FOR CHEMICAL PROTEOMICS AND DRUG TARGET IDENTIFICATION

by

DOINA MARIANA MIHAI

A dissertation submitted to the Graduate Faculty in Chemistry in partial fulfillment of the requirements for the degree of Doctor of Philosophy, The City University of New York

2011

© 2011

Doina Mariana Mihai

All Rights Reserved

This manuscript has been read and accepted for the Graduate Faculty in Chemistry in satisfaction of the dissertation requirement for the degree of Doctor of Philosophy

_____	_____
Date	Dr. Akira Kawamura, Chair of Examining Committee
_____	_____
Date	Dr. Mahesh K. Lakshman, Executive Officer

_____

Dr. Klaus Grohmann

_____

Dr. Themis Lazaridis

_____

Dr. Haiteng Deng
Supervisory Committee

THE CITY UNIVERSITY OF NEW YORK

Abstract

Benzophenone photoprobes for chemical proteomics and drug target identification

by

Doina Mariana Mihai

Advisor: Dr. Akira Kawamura

Benzophenone photoprobes are widely used in photoaffinity-labeling studies, especially for the characterization of ligand-receptor interaction. Photolabeling studies using benzophenone, however, are by no means routine experiments. It is not uncommon that carefully designed photoligands fail to label target proteins. In order to get insights into the important factors that affect the photolabeling efficiency, we conducted a structure-activity relationship study (SAR) on adenine-benzophenone photoligands. The study suggested that conformational flexibility was the determining factor that controls the photolabeling efficiency by benzophenone photoprobes.

In theory, photoaffinity-labeling can also be used for target identification of small molecules. However, the complexity of proteins in biological samples, such as cell lysate, tissue homogenates and serum samples, limits the use of benzophenone photoprobes in drug target identification and chemical proteomics. By using so called “blocking strategy” we were able to systematically classify the list of proteins identified from photoaffinity-labeling studies using benzophenone. The findings of this study enabled us to refine the experimental protocol for drug target identification and chemical proteomics using benzophenone photoprobes.

During the affinity purification of phochemically biotinylated proteins, we discovered that monomeric avidin resin can selectively enrich heat shock proteins (Hsps) from complex proteomes. Although such serum Hsps or circulating Hsps, has been linked to various diseases, including cancer and cardiovascular diseases, their characterization have been hampered be the abundant proteins in serum such as albumin and immunoglobulings. The development of simple and reproducible method for Hsp enrichment opens a new opportunity to define the roles of circulating Hsps in various diseases.

Acknowledgments

The support and encouragement of many people have contributed to this PhD thesis.

Foremost, I would like to express my sincere gratitude to my advisor, Dr. Akira Kawamura for his guidance, patience and support throughout my PhD. With his enthusiasm, his immense knowledge and his great efforts to explain things clearly, helped me better grasp the biochemistry aspects of my research project.

Special thanks to all my committee members, Dr. Klaus Grohmann, Dr. Themis Lazaridis, Dr. Haiteng Deng for their time and helpful suggestions during the annually committee meetings. In particular, I would like to thank Dr. Haiteng Deng for his help with mass spectrometry experiments and all his valuable suggestions. Extended thanks to Dr. Klaus Grohmann for always listening and giving me precious advices.

I would like to thank Carolina Salguero, Olga Aminova, Laurence James and Cha Kwang Won for their help with my research project. Additional thanks go to Dr. Sagit Hindi for helping me with the experiments and protocols at the beginning of my PhD. My warmest thanks to Dr. Maria Iacovidou and Anna Takaoka for being great friends and making my years in the lab particularly enjoyable. Thanks also to Dr. Tal Hasson for his help with HPLC experiments and for making sure I never get bored in the lab.

I would also want to thank Dr. Robert Nolan, Dr. Emmanuel Chang, especially Dr. William Grossman for serving on my proposal committee and for all the helpful suggestions.

I would like to thank Dr. Frida Kleiman's and Dr. David Foster's lab for providing us the cancer cell lines. Special thanks to Dr. Murat Cevher for his technical help and being an exceptional friend.

My graduate studies would have not been the same without all the support and friendship provided by all the Romanian people in Hunter College. I am particularly thankful to my friend, Dr. Gabriela Smeureanu for helping me apply to The Graduate Center and always helping me with all the paper work.

I would like to sincerely thank my best friends, Oana Pascal, Adelina Labau and Bogdan Dulu, for helping me get through the difficult times, and for all the emotional support, entertainment and caring they provided. Special thanks to Coca and Daniel Bouru for being like a family to me and helping me during the first years in New York City.

I am deeply indebted to my special friend Abhishek Jain for keeping me sane, helping me smile and also for his understanding, endless patience and encouragement when it was most required. Thank you Abhishek for believing in me and for the precious memories along the way.

Finally, and most important, I am deeply grateful to my wonderful family in Romania. My brother Florian, my sister-in-law Claudia and my nephew Razvan-Florian have always been very supportive and encouraged me to pursue my dreams. I dedicate this work to my parents, Stefana and Nicolae, who have stood by me and supported every choice I made, through unconditional love and confidence in my abilities. They deserve far more credit than I can ever give them. I miss and love you all very much!!!

Dedicated to my parents, Stefana and Nicolae Mihai for their never-ending support and love.

Dedicata parintilor mei, Stefana si Nicolae Mihai, pentru tot suportul si dragostea lor.

Table of Contents

List of Figures

List of Schemes and Tables

List of Abbreviations

Å	angstrom
ATP	adenosine triphosphate
Bpa	*p*-benzoyl-phenylalanine
C	carbon
CA125	cancer antigen 125
Calu1	lung cancer cell line
DCC	*N,N*'-dicyclohexylcarbodimide
DCM	dichloromethane
DCU	dicyclohexylurea
DMF	dimethylsulfoxide
DTT	dithiothreitol
EC_{50}	half-maximal effective concentration
ESI	electrospray ionization
Fmoc	9-fluorenylmethoxycarbonyl
Glo1	glyoxalase 1
H	proton
H_2O	water
HDAC	histone deacetylase
HeLa	cervical cancer cell line
HOBT	1-hydroxybenzotriazole

HPLC	high performance liquid chromatography
HRP	horseradish peroxidase
Hsp	heat shock protein
LC	liquid chromatography
LTA4H	leukotriene A4 hydrolase
MCF 7	breast cancer cell line
MeOH	methanol
mg	milligram
MHz	megahertz
min	minutes
mL	milliliter
mm	millimeter
MPs	metalloproteases
MS	mass spectroscopy
NMR	nuclear magnetic resonance
PDB	protein data bank
PDVF	polyvinylidene fluoride
PEG	polyethylene glycol
PNA	peptide nucleic acid
PSA	prostate-specific antigen
SAHA	suberoylanilide hydroxamic acid
SAR	structure-activity relantionship study

SDS-PAGE	sodium dodecyl sulfate polyacrylamide gel electrophoresis
T24	bladder cancer cell line
TBS	tris buffered saline
TBS-T	tris buffered saline with 1% tween 20
TFA	trifluoroacetic acid
THP1	human monocytic leukemia cell line
TIS	triisopropylsilane
µg	microgram
µl	microliter

Chapter I

Applications of benzophenone photoprobes for biomedical research

I.1 Common applications of benzophenone photoprobes

Benzophenone photoprobes are extensively used in biomedical research. One of the earliest applications of benzophenone photochemistry was pioneered by Breslow and co-workers in the early 1970's, in which benzophenone was used for the remote-oxidation of steroids.[1] Since then, photochemistry using benzophenone photoprobes has been employed for various biomedical applications.[2, 3] In particular, however, benzophenone photoprobes have been most extensively employed for the characterization of ligand-receptor interactions, in which photocrosslinkning is used to elucidate ligand binding sites and orientations. It is generally believed that benzophenone rapidly photocrosslinks amino acid residues within ~3.1 Å of the carbonyl oxygen, in which an inert C-H bond near the benzophenone carbonyl group is activated by hydrogen abstraction and then a covalent bond forms through a carbon-carbon radical coupling -reaction (Figure I.1).[2, 3] Photoaffinity-labeling using benzophenone has been employed to study ligand-receptor interactions of a wide variety of systems, such as ATP binding sites on ATPases,[4-18] lipid binding motifs on membrane proteins,[19, 20] and peptide-receptor interactions (Figure I.2).[21-23]

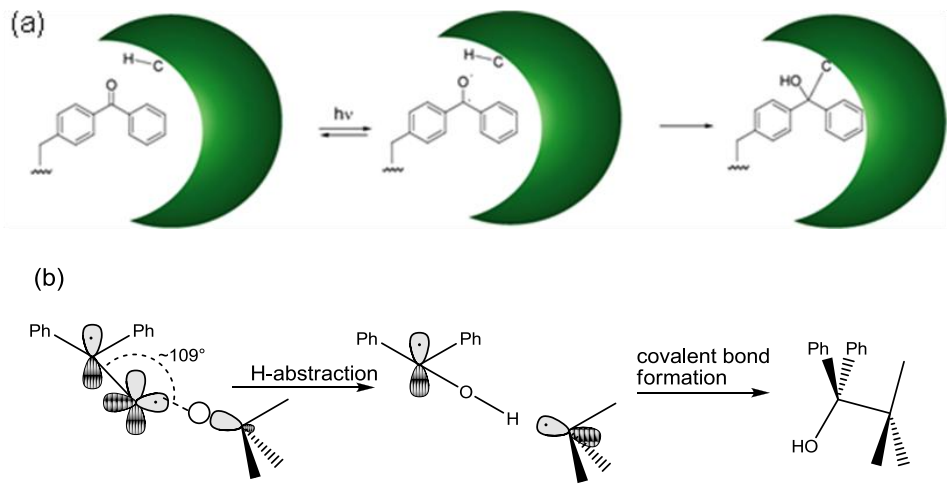

Figure I.1. Biochemistry of benzophenone. (a) Radical formation and covalent attachment to the target protein. (b) Stereoelectronic requirements for H-abstraction and covalent bond formation.

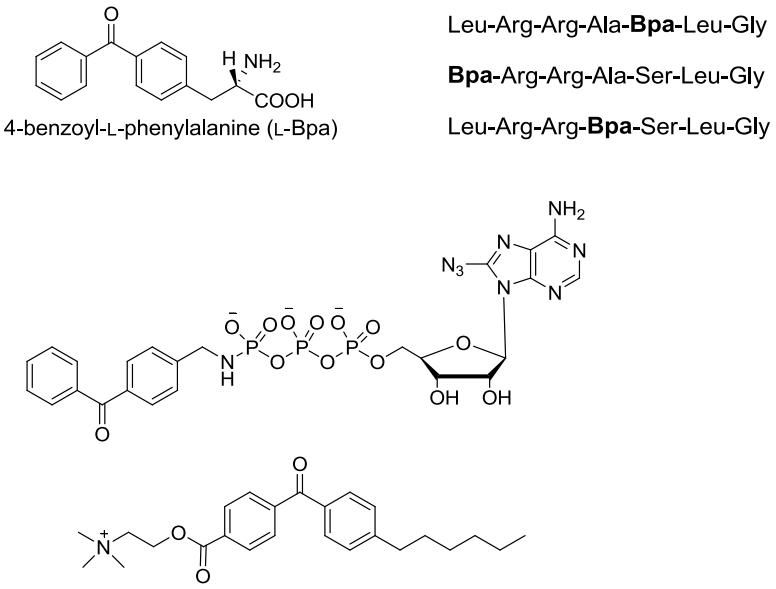

Figure I.2. Examples of benzophenone photoligands used for the characterization of protein-ligand interactions.[7, 13, 14, 24]

I.2 Expanding the scope of photoaffinity-labeling studies using benzophenone

In theory, photoaffinity labeling can be used for the purpose of drug target identification and chemical proteomics, although such applications are much rarer compared to the studies on ligand-receptor interactions. If benzophenone photoligands are conjugated with detection tags, such as biotin, benzophenone photoprobes can be used to selectively tag their target proteins in complex proteomes. Then tagged proteins can be detected and/or purified through the detection tags for identification. In fact, there are several recent examples in which benzophenone photoprobes are used to profile certain families of proteins in complex proteomes. For example, Saghatelian *et al* developed a photoreactive probe that targets metalloproteases (MPs).[25] MPs are an extremely large and diverse group of enzymes implicated in many physiological and pathological processes including peptide hormone signaling, tissue remodeling and cancer.[26-28] The HxBP-Rh photoprobe containing zinc-chelating hydroxamate, benzophenone and rhodamine tag (Figure I.3) was found to selectively label several active MPs in cell/tissue proteomes but not their zymogen or inhibitor-bound forms.

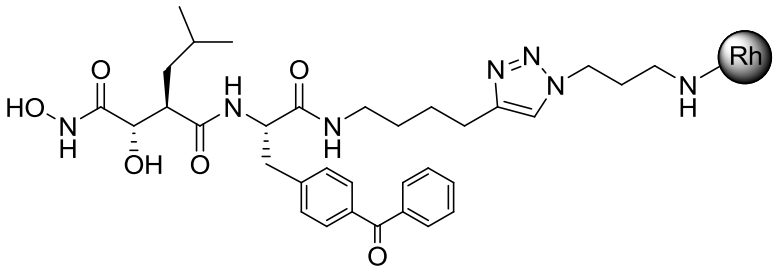

Figure I.3 Structure of HxBP-Rh photoprobe.[25]

Salisbury and Cravatt developed a photoreactive probe, SAHA-BPyne, for profiling histone deacetylases (HDACs) in complex proteome.[29] The reversible acetylation of lysine residues on histone proteins plays an important role in transcriptional activation and is catalyzed by histone acetyltransferases (HTAs) and HDACs, respectively. Class I and II HDACs are zinc-dependent metallohydrolases. Inhibitors of HDACs have been shown to induce differentiation in cancer cell lines and reduce tumor volume *in vivo*.[30, 31] The photoprobe was designed based on the scaffold of a general HDAC inhibitor, suberoylanilide hydroxamic acid (SAHA), by introducing benzophenone for covalent labeling of proximal proteins and alkyne group for click chemistry based tagging (Figure I.4). The SAHA-BPyne photoprobe was found to target multiple class I and II HDACs in proteomes as well as several HDAC-associated proteins.

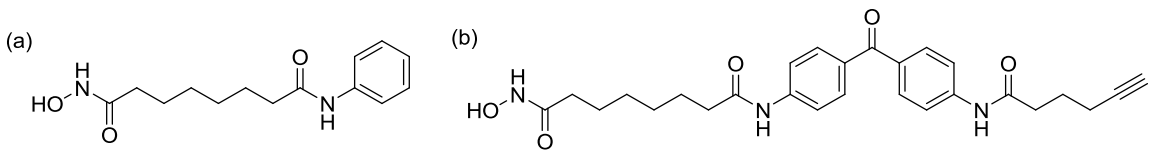

Figure I.4. Structures of (a) SAHA and (b) SAHA-BPyne photoprobe.[29]

However, there have been only few applications of benzophenone photoprobes to chemical proteomics and drug target identification. While many papers report the synthesis of benzophenone photoprobes for target identification,[25, 29, 32-45] only few studies have reported successful target identification.[29, 40] There are several possible reasons for this. First, close examinations of literature as well as our preliminary studies

suggest that the efficiency of photoaffinity-labeling is not quite as high as generally believed. In fact, photolabeling with benzophenone is by no means a routine experiment. Sometimes photoprobes fail to photocrosslink their target proteins even when they have been shown to bind to their targets through biochemical analyses, such as enzyme inhibitory assays, etc. This is a major problem if benzophenone photoprobes are to be used for chemical proteomics and drug target identification, because, in those applications, it is necessary to maximize the photocrosslinking efficiency so that photoprobes tag as many binding targets as possible for further characterization. Despite the extensive use of photoaffinity labeling studies using benzophenone photoprobes there has been no systematic study to identify the important factors that control the photolabeling efficiency. In Chapter II we present a structure-activity relationship study (SAR) on benzophenone photoligands for Lck, which examined the factors that can possibly affect photolabeling efficiency. The study suggested that binding affinity, as indicated by K_m, K_i, IC_{50}, etc., does not necessary correlate with the photolabeling efficiency. Instead, conformational flexibility of photoligands turned out to be the key factor that controls the photolabeling efficiency of benzophenone photoprobes. This is an important finding that should be taken into account when benzophenone photoprobes are designed for chemical proteomics and drug target identification in the future.

Another major problem that hinders the use of benzophenone photoprobes in drug target identification and chemical proteomics stems from the enormous complexity of proteins in biological samples, such as cell lysates, tissue homogenates and serum samples. Here, the ability of benzophenone photoprobes to form covalent bonds to their targets is both an advantage and a disadvantage. While they can be used to identify the

targets of modest affinity ligands, they tend to identify a large number of proteins when used in cellular and tissue samples. Deconvolution of potential target proteins, therefore, is necessary when benzophenone photoprobes are used in drug target identification. There is, however, no general approach to classify potential target proteins. As described in Chapter III, we employed what we call "blocking strategy" to successfully classify photolabeled proteins identified from a photoaffinity-labeling study of cell lysates. The findings from this study led us to refine the experimental protocol for drug target identification and chemical proteomics using benzophenone photoprobes.

Our studies on benzophenone photoprobes also led to an unexpected finding with potentially important biomedical implications. During the affinity purification of photochemically biotinylated proteins, we discovered that monomeric avidin resin can selectively enrich heat shock proteins (Hsps) from complex proteomes. This is an important finding because the method can be applied to profile and characterize minute quantities of Hsps in the blood serum. Although such serum Hsps, or circulating Hsps, have been linked to various diseases, including cancer and cardiovascular diseases, [46-52] their characterization has been hampered by the abundant proteins in the serum, such as albumin and immunoglobulins. The finding of this unique ability of monomeric avidin is described in Chapter IV.

Chapter II

Structural requirements for efficient photocrosslinking by benzophenone photophore

II.1 Introduction

Benzophenone is one of the most widely used photophore in photoaffinity labeling studies, particularly for the characterization of ligand-receptor interactions.[2, 3, 53] Extensive use of benzophenone can be explained by its commercial availability and compatibility with peptide-synthesis methodologies, including solid-phase synthesis. It has a higher chemical stability compared to other photoaffinity-labeling reagents, such as diazo esters, aryl azides and diazirines. Benzophenone can be manipulated in ambient light and can be activated by irradiation at ~350-360 nm, thus avoiding the protein-damaging wavelength. Furthermore, benzophenone reacts preferentially with C-H bonds, in the presence of water and other nucleophiles.[53-56]

Photolabeling studies using benzophenone, however, are by no means routine experiments. It is not uncommon that carefully designed photoligands fail to label target proteins. The outcome of photolabeling experiments can depend on a number of factors. Binding-affinity, as assessed by K_d, K_i, IC_{50} etc., is commonly used to select and optimize benzophenone probes for photocrosslinking experiments. But binding does not necessarily guarantee photolabeling. There are some notable discrepancies between binding-affinity and photolabeling efficiency in some studies. For example, in the study of benzophenone probes for histone deacetylases, the enzyme inhibitory potency was not indicative of the photolabeling efficiency.[45] A similar discrepancy between binding-affinity and photolabeling efficiency has been noticed in a study of secretin analogs containing benzophenone.[57] There are, therefore, additional factors that affect photolabeling efficiency.

Conformational flexibility of benzophenone photoligands may be an important factor affecting the specificity and efficiency of photolabeling.[2, 53] Conformational restriction can decrease the rate of photochemical reactions as evidenced by a series of studies on intramolecular photoreactions of benzophenone derivatives.[58, 59] But, too much flexibility can result in indiscriminate photolabeling and compromise the specificity. In the studies of ligand-receptor interactions, when specificity of labeling is important, photoprobes are designed to minimize flexibility in order to accomplish site-specific labeling.[60] On the other hand, for the chemical proteomics studies, when high efficiency of photolabeling is required, increased flexibility around benzophenone might be beneficial. The importance of conformational flexibility has not been systematically studied for intermolecular photoreactions, such as photoaffinity-labeling of protein targets by benzophenone photoligands.

In order to gain an insight into the importance of conformational flexibility in benzophenone photolabeling, we conducted a structure-activity relationship (SAR) study of our adenine-benzophenone photoligand **1S** (Figure II.1.a),[61] a simple conjugate of adenine, benzophenone and biotin. Our previous studies showed that this compound efficiently photolabeled recombinant Lck kinase, which is a Src-family kinase involved in a variety of physiological and pathological processes, including thymocyte differentiation, T-cell activation, lymphocyte malignancy and immunodeficiency.[62-66] The photocrosslinking site on recombinant Lck protein was mapped to either Gly383 or Leu384 in a hydrophobic pocket near the ATP-binding site.[61] Identification of the photocrosslinking site enabled us to build a model of photoligand-Lck complex (Figure II.1.b). The model suggested that the *pro*-R hydrogen of the central glycine moiety of **1S**

was exposed to the solvent. Thus, it seemed possible to replace this glycine moiety with D-amino acids without negatively affecting the existing interaction between Lck and **1S**. Six new adenine-benzophenone photoligands with varying conformational flexibility, therefore, were designed, synthesized and characterized by chemical and biochemical methods.

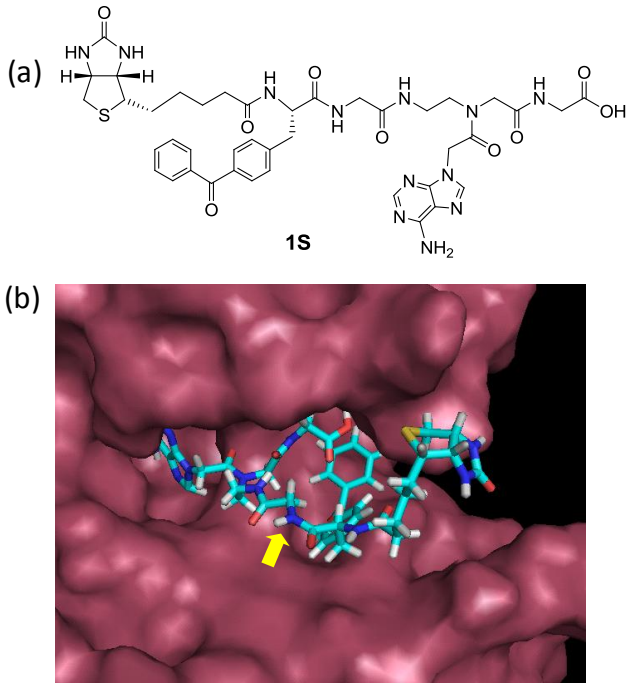

Figure II.1. (a) Structure of Lck-photoligand (b) The model of Lck-photoligand complex. The central glycine moiety is highlighted by the yellow arrow.

As described in detail in the following sections, this SAR study shows that conformational flexibility is indeed a critical factor for efficient photolabeling of Lck protein by adenine-benzophenone photoligands. The biochemical implications of our finding are discussed.

II.2 Design and synthesis of new adenine-benzophenone photoligands

Using our current model of adenine-benzophenone photoligand complex we designed and synthesized a new set of probes with a modified peptide backbone connecting the adenine, benzophenone and biotin moieties (Figure II.2). All the new probes were synthesized manually using a standard Fmoc chemistry on solid phase as illustrated in Scheme II. 1.[67] Their structures were confirmed by MS and NMR.

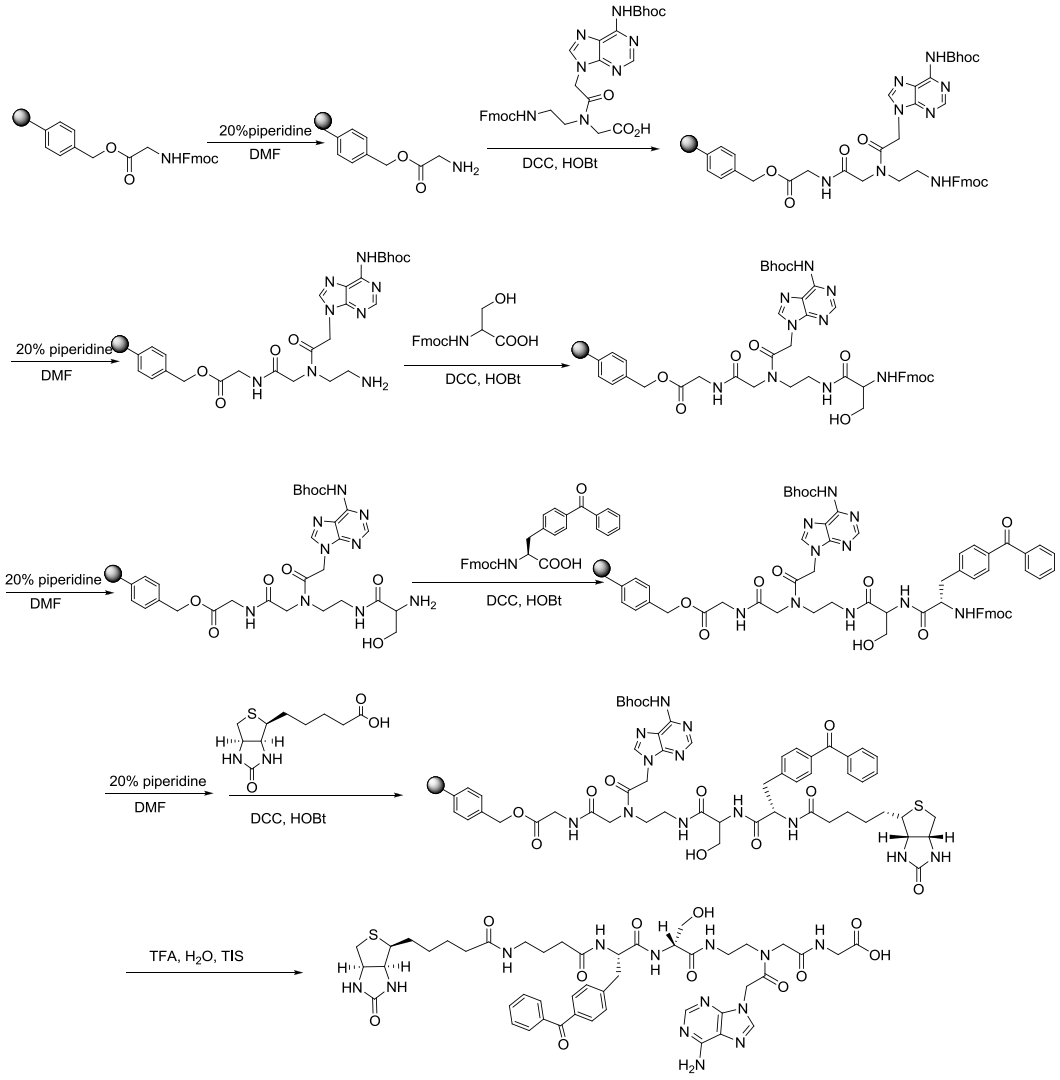

Scheme II.1. Solid phase synthesis of *Ser* photoligand.

Compound **1** (*Gly* ligand) contained the original adenine-benzophenone framework consisting of *p*-benzoyl-L-phenylalanine (Bpa), Gly, PNA-adenine, and Gly. It was essentially the same as the prototype **1S** except that there was a γ-aminobutyric acid (GABA) group between the biotin and benzophenone moieties. The longer linker allowed the use of streptavidin-horseradish peroxidase (HRP) instead of anti-biotin HRP conjugated antibody for more sensitive detection of photolabeled Lck protein. All new adenine-benzophenone photoligands contained this GABA spacer for the same reason. Compounds, **2** (*Ser* ligand) and **3** (*Glu* ligand) were obtained by replacing the glycine moiety between Bpa and PNA-adenine by D-Serine and D-Glutamic acid, respectively. Based on the computational modeling analysis, it was possible that these modifications could result in additional hydrogen bonds to Lck. While such extra hydrogen bonds could increase the binding affinity, they could reduce conformational flexibility of the bound ligands. These probes, therefore, could help us examine the relative importance between binding affinity and conformational flexibility: **2** and **3** would photolabel Lck better than **1** if binding affinity is the key factor for efficient photolabeling. Compounds **4** (*Pro* ligand) and **5** (*Pip* ligand), containing cyclic D-amino acids, were designed to evaluate the effects of conformational restriction imposed on the ligand backbone. By pre-organizing the probe to binding conformation we postulated that probes could improve binding affinity by lowering the entropic loss in the formation of Lck-probe complex. Again, **4** and **5** would photolabel Lck better than **1** if binding affinity is the key factor for efficient photolabeling. Compound **6** (*GABA* ligand) containing γ-aminobutyric acid in the place of the central glycine, was designed to assess the effects of enhanced

conformational flexibility. **6** would photolabel Lck better than **1** if conformational flexibility is the dominant factor for efficient photolabeling.

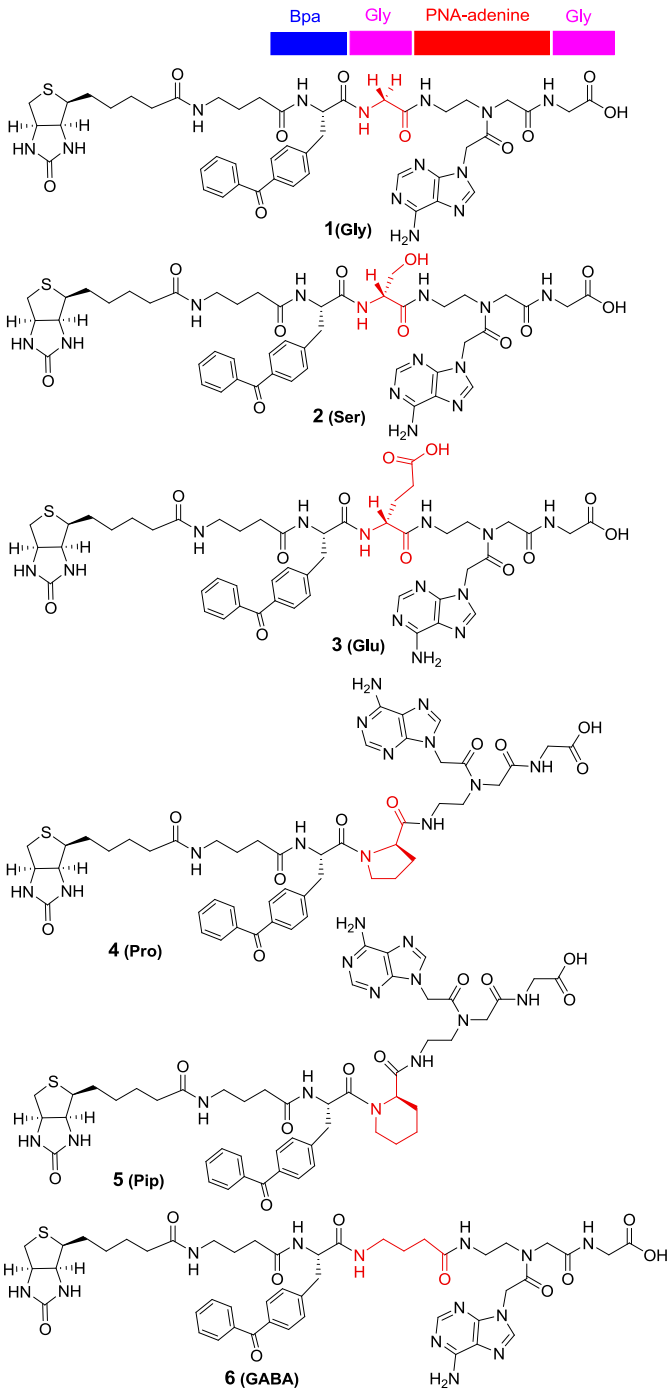

Figure II.2. Structures of the newly synthesized Lck ptotoligands.

II.3 Photocrosslinking efficiency

Binding efficiency of each probe was evaluated using recombinant Lck. The kinase-probe mixtures were irradiated under a UV-A lamp (λ_{max}=350nm). The irradiated samples were separated by SDS-PAGE and blotted onto PVDF membrane. Blotted membrane was treated with streptavidin-HRP conjugate and visualized by the Immobilon™ Western-chemiluminescent HRP reagent. Biotinylated Lck protein was visualized with Bio-Rad Chemidoc gel documentation system.

To quantify the photolabeling efficiency of new photolignads we calculated the half-maximal effective concentration (EC_{50}), that is the ligand concentration at which 50% of the maximum labeling was observed (Figure II.3 a). The EC_{50} was obtained by plotting the intensities of the bands observed from photolabeling of Lck with different concentrations of each probe against probe concentration. Among all the photoligands, the most flexible one, *GABA* ligand, tagged Lck most efficiently (EC_{50} = 4.4 µM). *Gly* ligand labeled efficiently Lck with the EC_{50} of 14.4 µM. On the other hand, *Pro* and *Pip* ligands, did not label Lck efficiently (EC_{50} >150 µM). *Ser* and *Glu* gave EC_{50} values of 23.3 µM and 18.4 µM, respectively, which were comparable to that of *Gly* ligand. While these results indicated that the conformational flexibility was indeed an important factor for efficient photolabeling, the lack of photolabeling by *Pip* and *Pro* could also be explained by other factors, such as lack of binding to Lck. Thus, a closer examination of the photolabeling process was necessary to clarify the key important factor for efficient photolabeling.

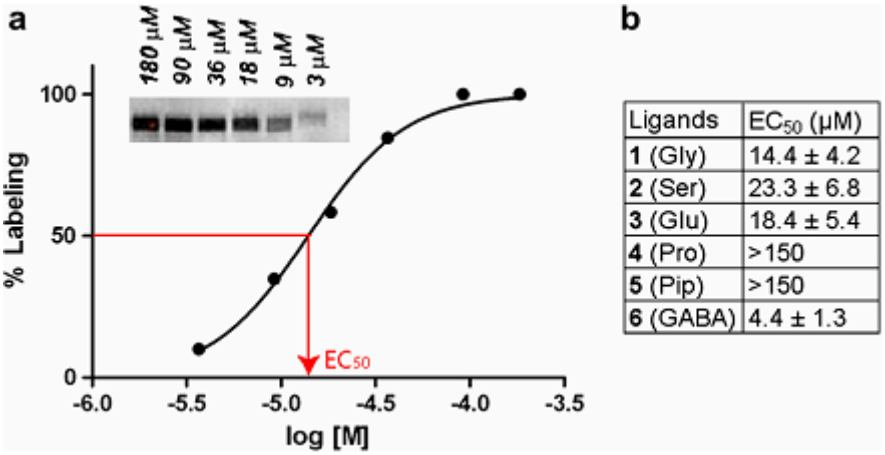

Figure II.3. Photoaffinity labeling study of newly synthesized Lck ligands. (a) The gel image of Lck tagged with different concentrations of 1, and the resulting titration curve, from which EC_{50} was estimated. (b) EC_{50} values of all photoligands: triplicate experiments (n=3) were made for each data point. "Reprinted from *Bioorg. Med. Chem.*, 16, Kawamura et al., 'Binding is not enough: Flexibility is needed for photocrosslinking of Lck kinase by benzophenone photolignads', p. 8824-29, Copyright (2008), with permission from Elsevier."[68]

The process of photolabeling involves two different steps: (1) initial ligand binding to Lck (non-covalent binding) followed by (2) photocrosslinking (covalent binding). It is also noted that the photolabeling of Lck competes with (3) probe decomposition due to intramolecular photoreactions (Figure II.4). At this stage, therefore, there were three possible reasons for the diminished labeling efficiency of the *Pro* and *Pip* probes:

(1) They did not bind to Lck.

(2) They bound to Lck but the bound ligands did not photocrosslink Lck.

(3) Their bent structures could facilitate intramolecular photochemical reactions.

In order to address the first possible explanation of the diminished labeling of the *Pro* and *Pip* ligands, binding affinity of individual probes was examined using a Lck kinase inhibition assay.

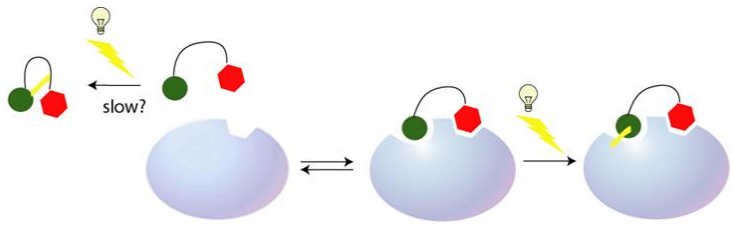

Figure II.4. Steps involved in the photolabeling of Lck. The red hexagon and green circle represent adenine and benzophenone, respectively. In photolabeling, a ligand first binds reversible to Lck, followed by the photocrosslinking reaction to form a covalent bond (yellow line). The photolabeling reaction can compete with the intramolecular reactions of the free photoligands.

II.4 Lck inhibition assay

The inhibitory activities of each probe were determined using a commercial kit, Promega Kinase-Glo® Plus Luminescent Kinase Assay. This assay uses luciferase to monitor unused ATP in kinase reactions. Since luminescence correlates with the amount of residual ATP, the signal is high when the kinase is inhibited.

This assay allowed us to estimate the relative binding-affinity to Lck of our probes, even though none of these compounds were potent inhibitors of Lck. The IC_{50} values of adenine-benzophenone photoligands are presented in Figure II.5. The kinase assay was revealing. *Ser* ligand (compound **2**) and *Pro* ligand (compound **4**) had the

lowest IC_{50} values (both ~50μM), therefore the highest affinity to Lck among all the photoligands. One possible explanation for these results could be that the rigidity of the linker between the adenine and benzophenone pre-organized the *Pro* ligand for target-binding, whereas *Ser* ligand could have additional hydrogen bonding interactions with Lck surface. On the other hand *Gly*, *Glu*, *Pip*, and *GABA* ligands had high IC_{50} values indicating a poor binding to Lck. These results indicated that D-Glu did not pick extra interactions with the protein, whereas the *Pip* ligand was fixed in a wrong conformation. The modest binding affinity of *GABA* ligand was expected because of its large conformational flexibility.

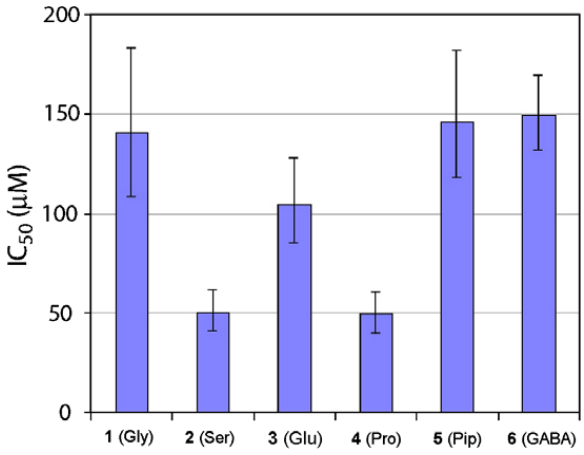

Figure II.5. The IC_{50} values of Lck photoligands. Lck kinase reactions in the presence and absence of photoligands were carried out on a 384-well plate. Following the incubation, residual ATP in each well was quantified with Promega Kinase-Glo® Plus Luminescent Kinase Assay. "Reprinted from *Bioorg. Med. Chem.*, 16, Kawamura et al., 'Binding is not enough: Flexibility is needed for photocrosslinking of Lck kinase by benzophenone photolignads', p. 8824-29, Copyright (2008), with permission from Elsevier."[68]

This kinase assay suggested that all probes could bind to Lck. Thus, the diminished photolabeling of Lck by the *Pro* and *Pip* probes could not be explained by the lack of binding: Possibility (1) above was eliminated at this stage. The results further suggested that conformational flexibility was an important factor for efficient photolabeling: The *Pro* and *Pip* probes did not photolabel Lck because they do not have enough conformational flexibility to undergo photocrosslinking reaction after binding to Lck. However, one other possibility was that the *Pro* and *Pip* probes could undergo intramolecular photoreactions and decompose much faster than other probes under UV light.

II.5 Decomposition of free photoligands under UV light

An HPLC method was used to evaluate the stability of free photoligands. The buffer solutions of ligands were irradiated under UV, and aliquots were taken at several time points to quantify the intact ligands by HPLC. After 30 minutes irradiation under a UV-A lamp, approximately 70-77% of photoligands remained intact (Figure II.6). Decomposition of the *Pro* and *Pip* ligands was not faster than others, thus it could not account for their diminished photolabeling efficiency.

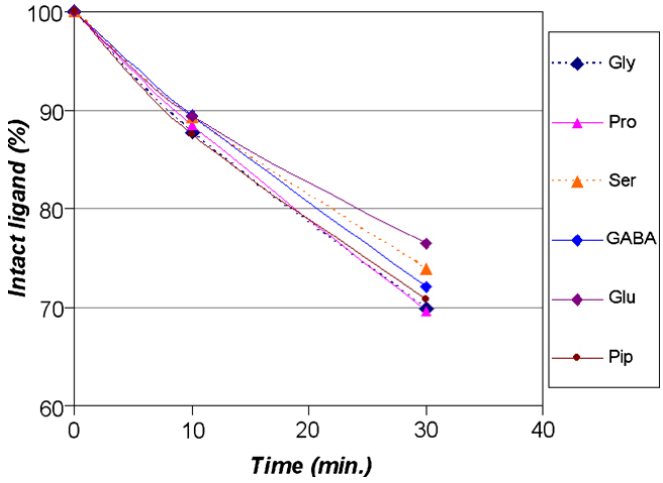

Figure II.6. Stability of photoligands under UV. Ligand solutions were irradiated under a UV-A lamp (kmax 350 nm). At different time points (0, 10, and 30 min), aliquots were taken and the amounts of intact ligand was quantified by HPLC (UV 280 nm). "Reprinted from *Bioorg. Med. Chem.*, 16, Kawamura et al., 'Binding is not enough: Flexibility is needed for photocrosslinking of Lck kinase by benzophenone photolignads', p. 8824-29, Copyright (2008), with permission from Elsevier."[68]

II.6 Discussion

Most studies on benzophenone photoprobes use biological preliminary data, such as K_d, K_i or IC_{50} etc., to show that the synthesized compounds bind to their intended targets.[36, 69-72] However, no study has systematically examined the issue of whether binding-affinity is predictive of successful photolabeling experiments. Our result indicates that binding between ligand and Lck is a necessary but not sufficient requirement for efficient photolabeling. A compound with high affinity could fail to label target proteins, whereas a compound with low affinity could still be a good photolabeling agent. Binding-affinity was not predictive of photolabeling efficiency in our system. Our

results, therefore, suggest that the selection and optimization of newly synthesized benzophenone photoligands should not depend only on their binding-affinity.

Instead of binding affinity, conformational flexibility was found to be the key factor that controls photolabeling efficiency. Overall conformational flexibility of our photoprobes correlated well with photolabeling efficiency. For example, the most flexible probe (*GABA* **6**) photocrosslinked Lck most efficiently, whereas conformationally restrained probes, such as *Pro* **4**, did not photolabel Lck even though they bind to the protein. There are several possible reasons why conformational flexibility is important for efficient photolabeling by benzophenone photoprobes.

First, photochemical reactions of benzophenone may require conformational flexibility at the lignad binding site. The photocrosslinking process by benzophenone involves multiple steps, namely, hydrogen abstraction, reorientation of benzophenone, and radical recombination to form the covalent bond with the protein surface. Using the *ab initio* calculation Severance *et al.* showed that the ideal C−O−H angle for hydrogen abstraction is 108.9° (Figure II.7 c).[73] After hydrogen abstraction minimal motion is necessary for benzophenone to fulfill the stereoelectronic requirements for C−C bond formation (Figure II.7 c).[53] Conformational restriction around the benzophenone moiety, therefore, can decrease the rate of photochemical reactions. In fact, similar observations were made in previous studies on intramolecular photoreactions of benzophenone derivatives.[58, 59, 74] It is likely that *GABA* photoligand can easily undergo conformational reorganization during photocrosslinking reaction (Figure II.7.a and c). Therefore, although *GABA* ligand does not bind to Lck tightly, it can still label Lck very efficiently. On the other hand, the conformational restriction of *Pro* and *Pip* photoligands prevented

the reorientation of benzophenone for radical recombination (Figure II.7.b). In the case of *Ser* ligand, hydrogen bonds with the Lck surface probably restricted the mobility of benzophenone in the bound ligand. Thus, the higher binding-affinity of *Ser* ligand did not result in enhanced labeling efficiency.

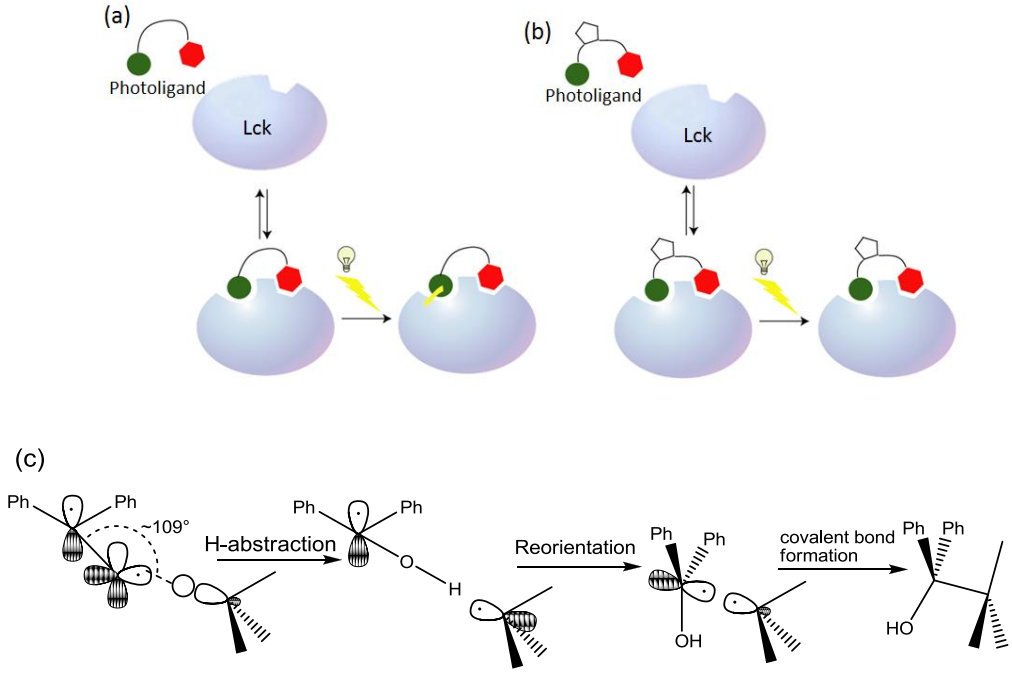

Figure II.7. Photochemical reactions of benzophenone may require conformational flexibility. The red hexagon and green circle represent adenine and benzophenone, respectively. (a) First, the photoligand binds reversible to the Lck, followed by photo-induced radical reaction. The flexible photoligands form a covalent bond (yellow line). (b) The photoligand binds reversible to the Lck, but the conformational constraint on the photoligand backbone prevents the photocrosslinking reaction. (c) Stereoelectronic requirements for H-abstraction and reorientation for C−C bond formation. Hydrogen abstraction occurs most efficiently when the C−O−H angle is 108.9°. Following the hydrogen abstraction, the benzophenone group has to reorient to form the C−C bond with the protein surface.

Second, photolabeling efficiency may be correlated with the surface area that can be accessed by the benzophenone group on the bound ligand. It is known that benzophenone preferentially photocrosslink amino acid residues that stabilizes radical intermediates, such as Met and Leu.[53, 75] Therefore, more flexible photoligand may have a higher chance of finding reactive amino acid residues before it dissociates from its target protein or before the photo-excited benzophenone goes back to the ground state. Thus, the photolabeling efficiency of the *GABA* probe was highest possibly because it had an access to a larger number of reactive amino acid residues on Lck surface (Figure II.8.a).

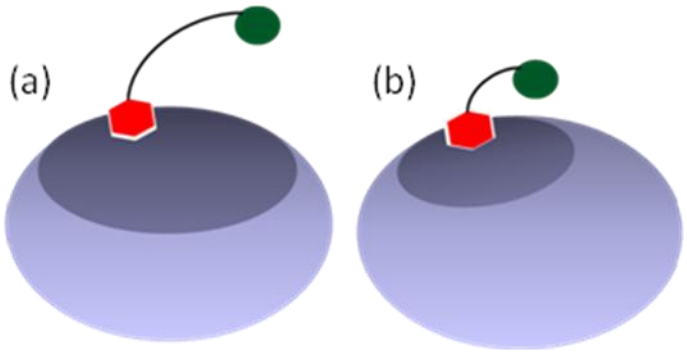

Figure II.8. Photolabeling efficiency may correlate with the protein surface areas that can be accessed by benzophenone. The red hexagon and green circle represent adenine and benzophenone, respectively. (a) More flexible linker allows search for reactive amino acid residues on a wider range of Lck surface. (b) Shorter linker limits the area that can be reached by benzophenone.

In conclusion, this study found that conformational flexibility was the determining factor for efficient photolabeling by our benzophenone photoligands. Too much flexibility, however, could result in the loss of specificity and random photolabeling. Although flexibility has been rarely considered in the past studies using

benzophenone photoligands, optimization of flexibility is an important issue that has to be taken into account when new benzophenone photoprobes are designed and synthesized. Synthetic schemes of benzophenone photoligands should allow the optimization of ligand flexibility so that desired photolabeling efficiency and specificity are attained for individual applications.

II.7 Experimental section

Materials

Fmoc-Gly-Wang resin, Fmoc-Gly, Fmoc-4-benzoyl-L-phenylaniline (Fmoc-L-Bpa), Fmoc-D-Bpa, dicyclohexylcarbodiimide (DCC), and 1-hydroxybenzotriazole (HOBt) were purchased from Fluka. Biotin-*N*-hydroxysuccinimide was obtained from Sigma-Aldrich. The Fmoc-protected peptide nucleic acid (PNA) adenine monomer, Fmoc-adenine-(Bhoc)-OH, was from Applied Biosystems. Laemmli sample buffer, Tris-glycine-SDS buffer, and streptavidin-horseradish peroxidase (HRP) conjugate were purchased from BioRad. Recombinant Lck kinase was obtained from Invitrogen. Millipore Immobilon™ Western-chemiluminescent HRP (ECL) substrate was obtained through Fisher Scientific. Kinase-Glo® Plus Luminescent Kinase Assay kit was purchased from Promega. Src tyrosine kinase substrate was obtained from Biomol. Greiner Bio-One Lumitrac 384-well plate (solid white) and 4-Amino-5-(4-phenoxyphenyl)-7H-pyrrolo[3,2-d]pyrimidin-7-yl-cyclopentane (the ATP-competitive Lck inhibitor; Calbiochem) were purchased through VWR Scientific. All other chemicals and solvents were obtained through Fisher Scientific and used without further purification.

Methods

Physicochemical analytical methods

NMR spectra were recorded on a Bruker Avance 500 MGHz spectrometer. Chemical shifts are reported in δ units (ppm) using the solvent peak as the internal standard. ^{1}H NMR splitting patterns are designated as singlet (s), doublet (d), triplet (t),

doublet of doublet (dd), and doublet of triplet (dt). Splitting patterns that could not be interpreted or easily visualized are designated as multiplet (m).

Mass spectral data were acquired on Agilent Technologies 1100 Series LC/MSD model G1946D using electrospray (ESI) ionization. Ionization was carried out with a drying gas temperature of 175 °C, a nebulizer pressure of 40 psi and a flow rate of 13 L/min. The mass range scanned was between 140 and 1000 amu with fragmentor values of 70 volts in negative ionization mode. The capillary was set to 4000 volts. Samples were introduced into the mass spectrometer using a 1:1 mixture of water and acetonitrile containing 0.1% acetic acid and 50 μM ammonium acetate. The flow rate of the solvent was 500 μl/min. Data was processed using Agilent's Chemstation software.

RP-HPLC was performed on an Agilent HPLC system equipped with an 1100 Diode-Array detector. Analytical RP-HPLC was performed using a Zorbax, Eclipse XDB-C8 (4.6 × 150 mm) column (5 μm). Semi-preperative HPLC was performed using Econosil C-18 10 u (10 × 250 mm). Separation was achieved using a linear gradient at a flow rate of 1 ml/min (Analytical HPLC) or 3ml/min (Semi-preparative HPLC) of Buffer **A** (20% MeOH), buffer **B** (100% MeOH), and 0.01% TFA. Column effluent was monitored by UV absorbance at 254, 220, and 280 nm. Elution Conditions: t = 0 min A = 100%, t = 5 min A = 100%, t = 20 min A = 50%, t = 30 min A = 0, t = 35 min A = 100%.

Chemical synthesis

Gly, Pro, Pip and *GABA* ligands were synthesized previously in our group. *Ser* and *Glu* ligands were synthesized during my thesis study as presented below. Probe synthesis was accomplished manually using a stepwise solid-phase procedure. All couplings were carried out over night in dimethylformamide (DMF) using a 2-fold excess (over resin loading) of protected monomer, activated with an equimolar of HOBt and DCC in room temperature. Reaction was monitored using the Kaiser test for free amines.[76] *N*-Fmoc group was removed using 20% (v/v) piperidine in DMF for 5 min followed by 20 min. Probes were removed from the solid support with simultaneous sidechain deprotection using a 95% trifluoroacetic acid (TFA), 2.5% triisopropylsilane (TIS) and 2.5% water solution for 2 h at room temperature. TFA was removed under reduced pressure. Crude material was precipitated and washed with cold petroleum ether. Probes were purified using semi-preparative HPLC, and the relevant fractions were collected and lyophilized. The purified probes were analyzed using analytical HPLC, MS, and NMR. The NMR spectra exhibited conformational isomerism at room temperature, which arise from the tertiary amide conformers at the PNA adenine moiety. The ^{1}H-NMR data given below are for the major conformers of the probes.

Probe 2 (*Ser* ligand) [Biotinyl-γ–aminobutyryl-p-benzoyl-L-phenylalanyl-D-serinyl-adenine-*N*^{9}-acetyl-(2-aminoethyl)glycinyl-glycine]

Fmoc-Gly-Wang resin (250 mg) was swollen in *N*-Methyl- Pyrolidone for 1 hour. The liquid was then removed and the resin was washed 3 times with DMF and 3 times with DCM/Methanol (1:1). To remove Fmoc group, the resin was washed with 20% piperidine

in DMF solution for 10 minutes, and then again with the same solution for 20 minutes. The resin was washed 3 times with DMF and 3 times with DCM/Methanol (1:1). The completeness of the reaction was checked by ninhydrin test. In the next step, Fmoc-PNA-Adenine (Bhoc)AEG-OH (272.2 mg, 2 eq), HOBt (50.7 mg, 2 eq) and DCC (77.4 mg, 2 eq) were dissolved in 2 ml DMF and the solution was cooled for 1h (0 °C). The precipitated dicyclohexylurea (DCU) was then removed and the solution was added to the resin. The mixture was shaken overnight. The liquid phase was removed and the resin was washed 3 times with DMF and 3 times with DCM/Methanol (1:1). The completeness of the reaction was checked by ninhydrin test. The Fmoc group was then removed as described above and Fmoc-D-Serine (143.75mg, 2 eq) was coupled using HOBt (50.7 mg, 2 eq) and DCC (77.4mg, 2 eq) as described above. Likewise, Fmoc-L-Bpa-OH (184.32 mg, 2 eq), Fmoc-γ-aminobutyric acid (Fmoc-GABA) (122.01 mg, 2 eq), and Biotin (91.62 mg, 2 eq), were coupled using the same DCC/HOBt coupling reaction. The product was cleaved from the resin by 10 ml of a 95 % TFA, 2.5 % TIS and 2.5 % water solution. The mixture was allowed to stand for 2 h, and then the volume of TFA was reduced by N_2. The precipitate was obtained in cold petroleum ether. The precipitate was collected under vacuum filtration. The total yield of the synthesis (11 steps) was 26%. The product was further purified using semi-preparative HPLC, and relevant fractions were lyophilized to give a white solid. Analytical RP-HPLC retention time: 16.05 min. ESIMS (expected m/z 1000.09) m/z 1002.00 (MH^+), 501.03 ($M_2H^+/2$). ^{1}H-NMR (500 MHz, DMSO) 8.64 (1H, t, NH), 8.48 (1H, m, NH), 8.25 (1H, s, CH), 8.20 (1H, s, CH), 8.04 (1H, m, NH), 7.75-7.20 (9H, m, 9×CH), 7.30 (2H, s, NH_2), 6.37 (2H, m, 2×NH), 5.20 (2H, m, CH_2), 4.55 (1H, m, CH), 4.40 (1H, m, CH), 4.32 (1H, m, CH), 4.18 (2H, m,

CH_2), 4.15 (1H, m, CH), 3.75 (2H, m, CH_2), 3.62 (2H, m CH_2), 3.44 (2H, m, CH_2), 3.26 (2H, m, CH_2), 3.20 (2H, t, CH_2), 3.08 (2H, m, CH_2), 2.90 (1H, m, CH) 2.75 (2H, m, CH_2), 2.30-2.20 (4H, m, 2×CH_2), 2.04 (1H, t, OH), 1.80 (2H, m, CH_2), 1.15-1.60 (6H, m, $CH_2CH_2CH_2$).

Probe 3 (*Glu* ligand) [Biotinyl-γ–aminobutyryl-p-benzoyl-L-phenylalanyl-D-glutamyl-adenine-N^9-acetyl-(2-aminoethyl)glycinyl-glycine]

Probe 3 (*Glu* ligand) was synthesized by the same procedure employed for the probe 2 (*Ser* ligand) except for the introduction of D-glutamic acid (159.55 mg, 2eq) between PNA-adenine and *p*-benzoyl-L-phenylalanine. The total yield of the synthesis (11 steps) was 36%. Analytical RP-HPLC retention time: 16.10 min. ESIMS (expected m/z 1042.12) m/z 1043.23 (MH^+), 522.06 ($M_2H^+/2$). ^{1}H-NMR (500 MHz, DMSO) 8.45 (1H, t, NH), 8.42 (1H, m, NH), 8.30 (1H, s, CH), 8.23 (1H, s, CH), 8.10 (1H, m, NH), 7.70-7.20 (9H, m, 9×CH), 7.27 (2H, s, NH_2), 6.30 (2H, m, 2×NH), 5.25 (2H, m, CH_2), 4.75 (1H, m, CH), 4.60 (1H, m, CH), 4.42 (1H, m, CH), 4.25 (1H, m, CH), 3.75 (2H, m, CH_2), 3.60 (2H, m CH_2), 3.54 (2H, m, CH_2), 3.36 (2H, m, CH_2), 3.22 (2H, t, CH_2), 3.10 (2H, m, CH_2), 2.80 (1H, m, CH) 2.65 (2H, m, CH_2), 2.47-2.35 (4H, m, 2×CH_2), 2.30-2.17 (4H, m, 2×CH_2), 1.82 (2H, m, CH_2), 1.20-1.60 (6H, m, $CH_2CH_2CH_2$).

Photolabeling of Lck and Western blot

0.5 µl aliquots of purified kinases were mixed with 1 µl of a probe solution (3.67 mM in DMSO). Photocrosslinking was carried out under six Sylvania 350 Blacklight lamps (15 W, λ_{max} 350 nm) for 2 h, in which samples were kept on ice and placed approximately 5 cm below the lamps. Following the photocrosslinking, samples were mixed with Laemmli Sample Buffer (BioRad) with 5% (v/v) 2- mercaptoethanol, denatured at 80 ºC for 5 min and separated on SDS-PAGE (5-20 % Tris-HCl gel, 200 V, 1 h) in 1× Tris-Glycine-SDS buffer (BioRad). Gel was blotted onto PVDF membrane (200 mA, 2h) in a cold transfer buffer (20% methanol in 1× Tris-Glycine buffer). Blotted membrane was blocked with 5% non-fat milk in Tris-buffered saline containing 1% Tween 20 (TBS-T) for 1 h. Blocked membrane was rinsed with TBS-T (5 min), treated with streptavidin-hoarseradish peroxidase (HRP) 17 µL in 3% non-fat milk in TBS-T) for 30 minutes, and washed with TBS-T (20 min × 3). The washed membrane was treated with the Immobilon™ Western-chemiluminescent HRP (ECL) reagent for 5 min. Bands were observed with the BioRad ChemiDoc gel documentation system.

Lck kinase assay

The inhibitory activities of individual photoligands were determined using Kinase-Glo® Plus Luminescent Kinase Assay (Promega). This assay utilizes luciferase to monitor unused ATP in kinase reactions; thus the signal is high when kinase is inhibited. Assays were performed per manufacturer's instructions. Briefly, 8 µl of 0.25 mM Src substrate peptide (Biomol) in a buffer (50 mM HEPES, pH 7.3, 2.5 mM DTT, 0.01%

Triton X-100, 10 mM $MgCl_2$) was added to each well of 384-well plate (Greiner Bio-One Lumitrac plate, solid white). 0.5 µl of Lck (Invitrogen, Part# P3043, Lot# 37621F), which had been prediluted in the buffer above to 46 ng/µl, and 0.5 µl of ligand at different concentrations were then added to each well. Kinase reaction was initiated by 1 µl of 100 lM ATP. After 1-h incubation at the room temperature, 10 µl of Kinase-Glo reagent was added to each well and incubated further for 10 min at room temperature. Luminescence of each well was measured by SpectraMax Gemini EM microplate spectrofluorometer (Molecular Devices). IC_{50} values and the 95% confidence interval (CI) of a mean were obtained by fitting the data from replicate trials (n = 2 or 3) to a sigmoidal dose–response curve using GraphPad Prism (Graph- Pad Software).

Measurements of probe decomposition under UV

The decomposition of probes under UV irradiation was monitored by RP-HPLC. One hundred microliters of each probe (30 µM) in the buffer was irradiated under six Sylvania 350 Blacklight lamps (15 W, λ_{max} 350 nm), in which samples were kept on ice and placed approximately 5 cm below the lamps. At various time intervals (t = 0, 10, and 30 min), aliquots were taken and examined by HPLC. Peak areas on chromatograms were used to estimate the intact probe concentrations.

Chapter III

Target deconvolution in photoaffinity-labeling using benzophenone photoprobes

III.1 Introduction

Benzophenone photoprobes are widely used in photoaffinity-labeling studies, especially for the characterization of ligand-receptor interactions. In theory, photoaffinity-labeling can also be used for target identification of small molecules. In fact, it may be the ideal (and perhaps the only) method to identify the targets of modest affinity ligands: It is difficult to use affinity purification for the target identification of modest affinity ligands. Photocrosslinking enables the covalent modification of the target protein in complex proteomes. If the photoprobe contains a tag for affinity purification, such as biotin, the modified (tagged) protein can then be purified and identified by mass spectrometry. In reality, however, benzophenone photoprobes are rarely used in drug target identification. Although there are several papers describing the synthesis of photoprobes for target identification,[25, 32-39, 41, 42, 44] only a few studies have actually reported successful target identification using benzophenone photoprobes.[29, 40] The obvious question is why benzophenone photoligands are not widely used for drug target identification.

One major problem is caused by the ability of benzophenone photoprobes to identify even the targets with modest binding affinity. When cellular and tissue samples are subjected to photoaffinity-labeling and mass spectrometric analyses, the resulting profiles are typically very complex, containing hundreds of potential target proteins. This is because photoaffinity-labeling identifies any proteins that have modest affinity to the photoprobe of interest. In addition, the list includes proteins that recognize structural motifs other than the drug of interest. For example, it is possible that some proteins

recognize benzophenone or tag (biotin, fluorophore, etc.). Even if the binding affinity is weak, those proteins will still show up on the list of potential targets.

Another issue is the lack of experimental methods to deconvolute the complex list of potential target protein. Although it is possible to narrow down the list based on MS scores and focus only on the proteins with high scores, the list can still contain potential targets that could not be expected based on the biological properties of the drug. Most studies focus on the proteins that can be explained based on the known chemical and biological properties of the drug of interest.[40] It is, however, important to characterize those "unanticipated" potential targets because they might constitute previously overlooked new targets of the drug. Even if they recognize motifs other than the drug of interest, such as benzophenone, the information is useful for future photoaffinity-labeling studies using benzophenone photoprobes. Besides, many clinical drugs, such as ketoprofen,[77] contain benzophenone or analogous frameworks. Thus, identification of proteins that recognize benzophenone could lead to the discovery of new targets of those drugs. It is, therefore, important to establish an experimental method to determine which structural element of the photoprobe is recognized by the potential target proteins.

To this end, my thesis study examined the utility of blocking strategy. Blocking strategy is a simple way to examine how a protein recognizes the benzophenone photoprobe of interest. The strategy is based on the assumption that photolabeling is blocked by the structural fragment recognized by the protein. If a protein recognizes the drug portion of the photoprobe, the photolabeling should be diminished in the presence of excess drug (Figure III.1.b). On the other hand, the photolabeling should not be affected when free benzophenone is used as the blocker (Figure III.1.c). Analogously, proteins

that recognize benzophenone or other parts of the photoprobe can be determined through a series of blocking experiments. Although the approach has been used in a few studies,[45, 78] it has not been employed to systematically classify the list of proteins identified from photoaffinity-labeling studies using benzophenone.

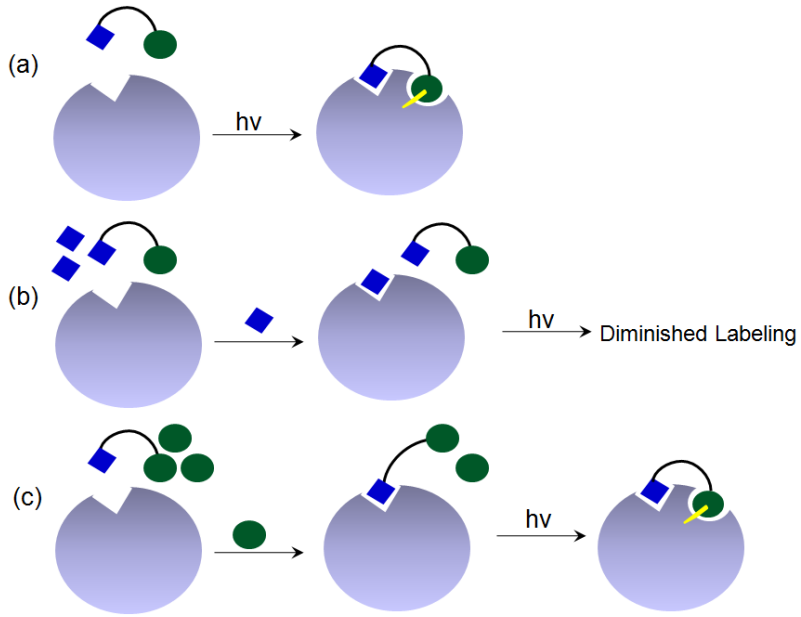

Figure III.1. Blocking strategy. The blue circle and blue diamond represent benzophenone and drug portion, respectively. (a) The benzophenone photoprobe covalently binds to protein (yellow line represents the covalent bond). (b) In the presence of excess drug the photolabeling is diminished. (c) Photolabeling is not affected in the presence of excess of benzophenone.

In order to test the utility of this blocking strategy, we conducted a photoaffinity-labeling study using adenine-benzophenone photoprobe. As described in the previous chapter, we have been developing adenine-benzophenone probes.[61, 68, 78] The structure of Bpa-Gly-PNAA-Gly was found to be a good framework for efficient photolabeling of

recombinant Lck protein. The finding set a stage to identify the real cellular targets in complex proteomes. To this end, we designed and synthesized a new generation of adenine-benzophenone photoligands that contain polyethylene glycol (PEG) linker between the benzophenone and biotin moieties (Figure III.2). The addition of PEG linker permits efficient affinity purification of photolabeled proteins from cell lysates by taking the advantage of the strong avidin-biotin interaction.[79-81]

This chapter presents photoaffinity-labeling of cancer cell lysates with our PEGylated adenine-benzophenone photoprobe, followed by the examination of the blocking strategy to classify some of the "unexpected" potential targets. Based on our previous studies as well as the structure of our photoprobe, the expected targets were adenine binding proteins, such as ATPase and kinases. However, some unexpected proteins were also identified in this study. A series of blocking experiments revealed previously overlooked off-targets of clinically used drugs (*vide infra*). Chemical and biomedical implications of our findings will be discussed.

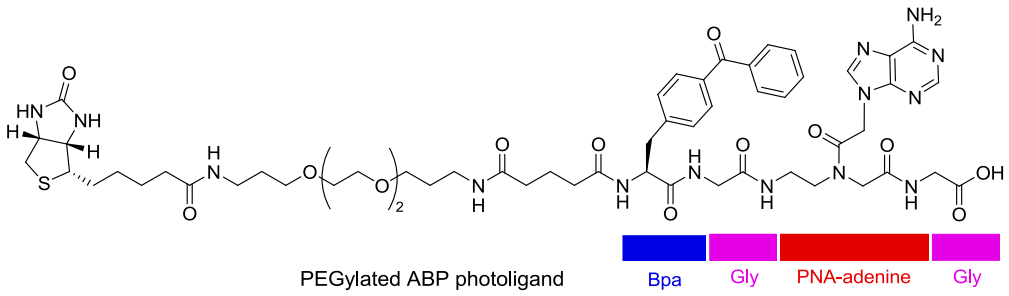

Figure III.2. Structure of PEGylated adenine-benzophenone photoligand.

III. 2 Probe synthesis

Probe synthesis was performed on solid phase support using standard Fmoc/Bhoc chemistry,[67] using SYMPHONY/Multiplex peptide synthesizer (RAININ-Instrument Co. Inc.), as shown in Scheme III.1. Starting with Fmoc-Gly-Wang resin, Fmoc was removed under basic conditions (20% piperidine in dimethylformamide (DMF)). *N*-(N^6-Bhoc-adenine-N^9-acetyl)-*N*-(2-Fmoc-aminoethyl)glycine(Fmoc-PNA-adenine(Bhoc)-OH) was coupled using *O*-Benzotriazole-*N,N,N',N'*-tetramethyl-uronium-hexafluoro-phosphate (HBTU) as the coupling reagent. Fmoc-Gly-OH, Fmoc-4-benzoyl-L-phenylaniline (Fmoc-L-Bpa), and *N*-biotinyl-NH-$(PEG)_2$-COOH were then coupled in that order using the same chemistry. Cleavage from the solid support and simultaneous sidechain deprotection were carried out using a mixture of 95% trifluoroacetic acid (TFA), 2.5% triisopropylsilane (TIS) and 2.5% water. Crude material was then purified by reverse phase HPLC and their structures were confirmed by NMR and mass spectrometry. The newly synthesized PEGylated photoprobe enabled us to conduct the photoaffinity-labeling studies using complex proteomes, such as cancer cell lysates.

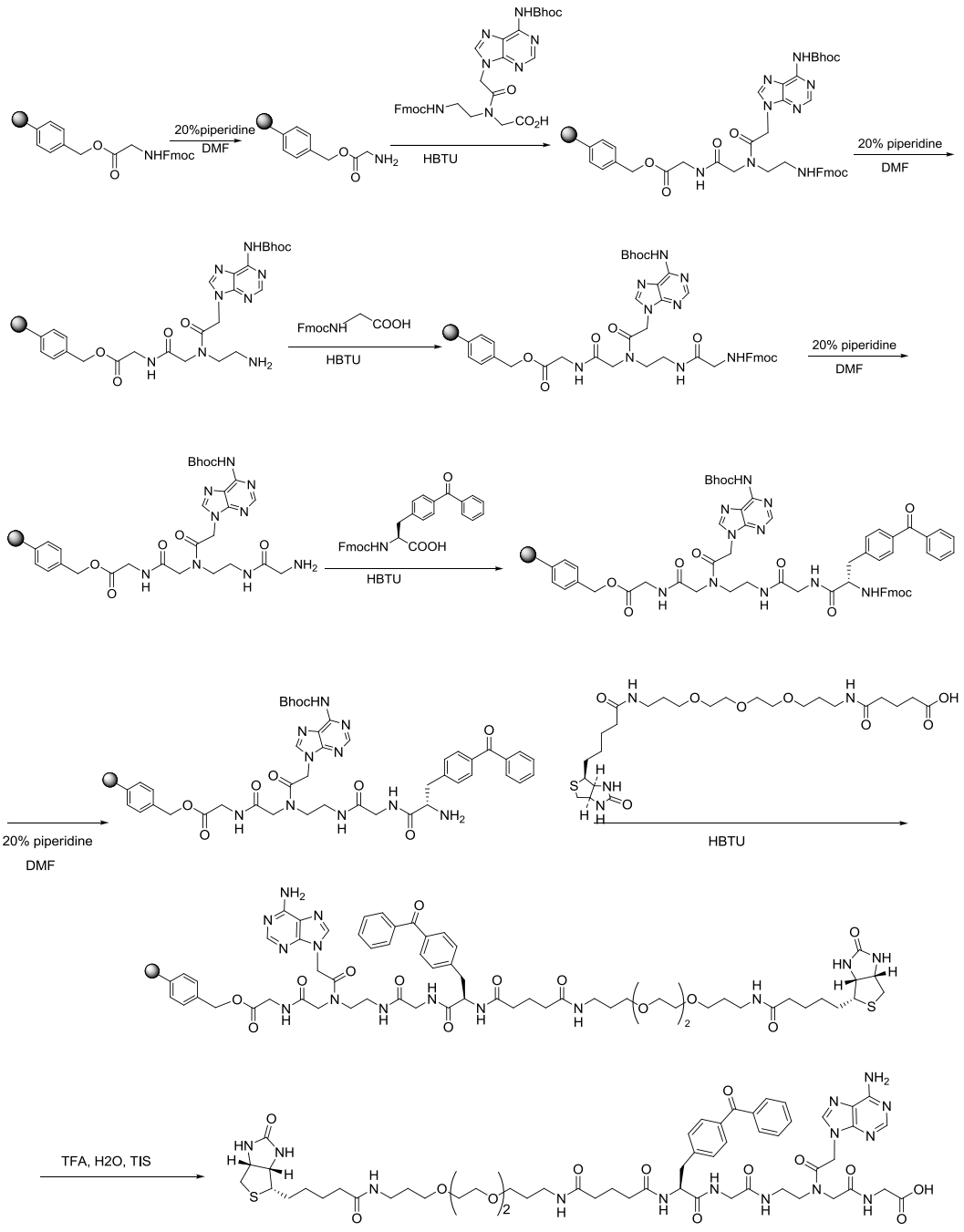

Scheme III.1. Solid phase synthesis of PEGylated adenine-benzophenone photoligand.

III.3 Cellular target identification

In order to identify a cancer cell line that expresses the protein targets of our photoprobe, we screened a panel of six different cancer cell lines, namely, Jurkat (T-cells),[82] THP1 (human mocytic leukemia cells),[83] HeLa (cervical cancer),[84] T24 (bladder cancer),[85] MCF7 (breast cancer),[86] Calu1(lung cancer)[87] (Figure III.3). Cell lysates were subjected to photoaffinity labeling, followed by SDS PAGE and Western blot. Biotinylated proteins were then visualized with streptavidin-HRP and chemiluminescence. For each cancer cell line, three experiments were carried out: (1) total cell lysate without photoaffinity labeling (background control), (2) total cell lysate with photoaffinity labeling (profile of photolabeled proteins), and (3) total cell lysate with photoaffinity labeling, followed by affinity purification using strepavidin-resin (profile of isolable photolabeled proteins). Although HeLa and MCF7 gave many photolabeled proteins, they could not be affinity-purified with streptavidin. On the other hand, THP1 lysate most reproducibly expressed large amounts of isolable photolabeled proteins. We, therefore, proceeded to identify the target proteins of PEGylated adenine-benzophenone photoligand in THP1.

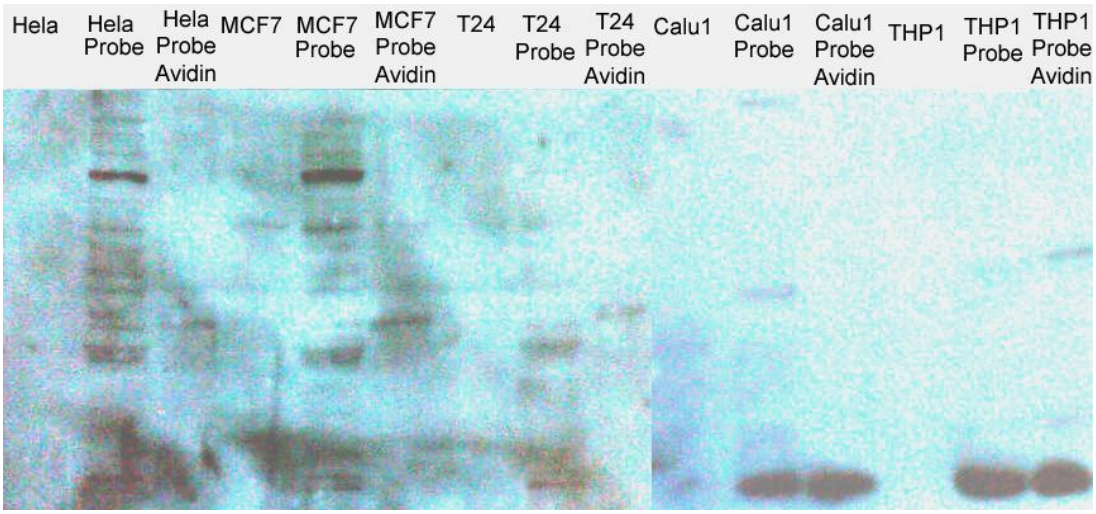

Figure III.3. Photolabeling of PEGylated photoligand with total cell lysate. Total lysate of different cancer cell lines were photolabeled with PEGylated adenine-benzophenone photoligand with and without avidin affinity purification.

In order to identify the photolabeled proteins by MS, it was necessary to conduct a large scale experiment, because MS-based protein identification usually requires the amounts of proteins that can be visualized with Coomassie blue stain. A large quantity of THP1 total lysate was prepared and incubated with PEGylated photoligand. Experimental steps followed the scheme outlined in Figure III.4. The protein-photoligand mixture was irradiated under a UV-A lamp (λ_{max}=350nm). The biotinylated proteins were then purified with strepavidin-agarose beads and separated by SDS-PAGE. Affinity-purified proteins were then visualized with Coomassie blue stain. The Coomassie stained bands were excised from the gel, digested with trypsin and the proteins were identified by peptide mass fingerprinting analysis, which matches the tryptic peptide masses in the mass spectrum to the calculated tryptic peptide masses of proteins in a database.[88]

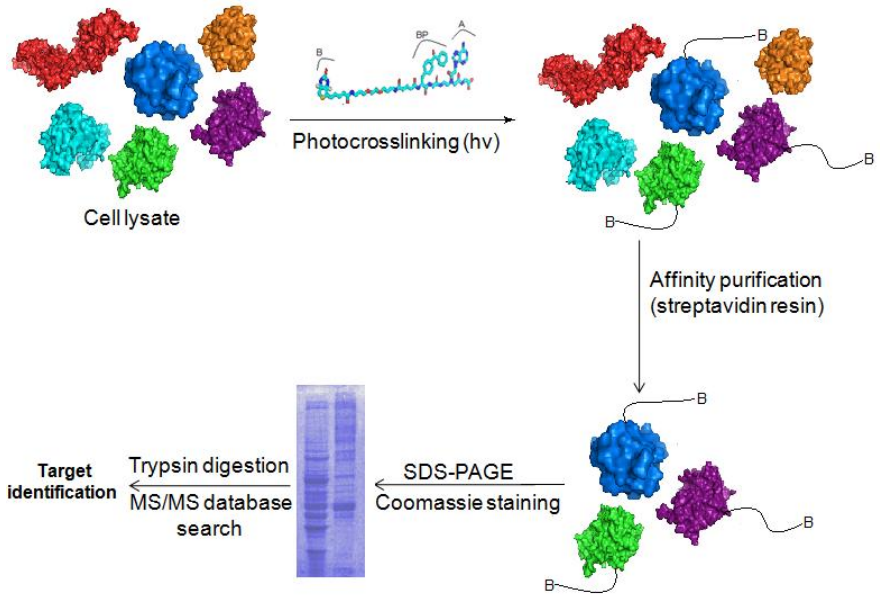

Figure III.4. Experimental procedure for identification of cellular targets from total lysate of THP1 cells.

III.4 Results and discussion

Proteomic profiling identified a total of 211 proteins with significance threshold $p < 0.05$ (Appendix 1). Table III.1 summarizes the proteins that had the high MASCOT scores in this experiment. Among the highest score proteins were classical adenine binding proteins, such as various actin isoforms, and nucleotide binding proteins, tubulin isoforms. These proteins were expected targets of our adenine-benzophenone photoprobe because they are known to be expressed abundantly in cells and recognize nucleotides. The list, however, also included leukotriene A4 hydrolase (LTA4H) and Glyoxalase 1 (Glo1), which had not been anticipated from the structure of our photoprobe.

Table III.1 High score target proteins identified by PEGylated photoligand

Score	GI	Mass	Gene
1387	2392338	20861	glyoxalase I
963	16359158	42078	actin beta
893	51247429	69652	leukotriene A4 hydrolase
791	4885049	42334	cardiac muscle alpha actin 1 preprotein
764	4501889	42249	actin gamma 2 propeptide
392	37492	50810	alpha-tubulin
145	9507215	50746	tubulin, alpha 8
138	5174735	50255	tubulin, beta2

Neither Glo1 nor LTA4H possess the typical nucleotide binding sequence but their scores in the proteomic profile were among the highest. Glo1 is a homodimeric zinc metalloenzyme that catalyzes the conversion of cytotoxic methylglyoxal to nontoxic hemithioacetal using glutathione as a cofactor (Figure III.5).[89, 90] Glo1 has been associated with various diseases including cancer,[91] diabetes[92, 93] and Alzheimer's disease.[94] Specific inhibitors of Glo1 have been sought as possible anticancer agents, by inducing elevated levels of methylglyoxal in cancer cells.[90, 95-97] In addition, Glo1 is considered as a potential target of malaria therapy.[98]

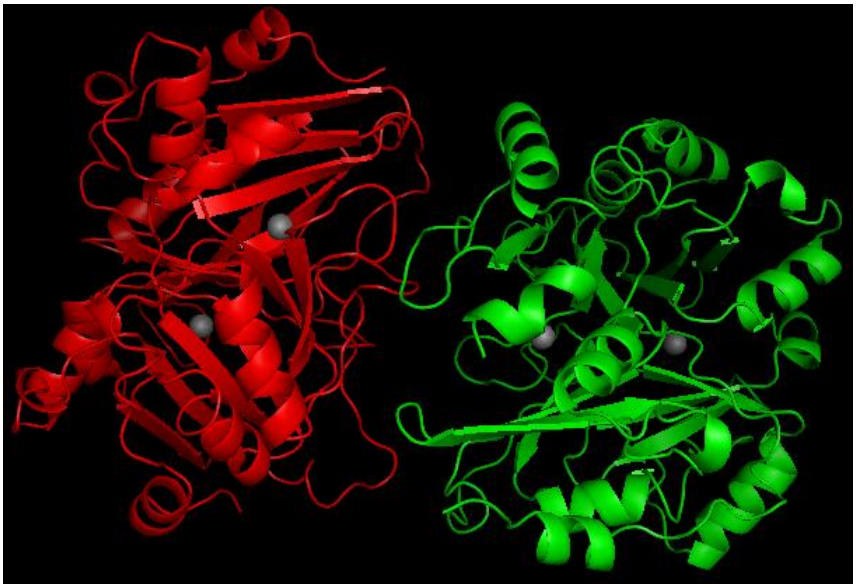

Figure III.5. Crystal structure of Glyoxalase 1 (PDB 1FR0). Glo1 is a ~21kDa homodimeric zinc metalloenzyme. Catalytic Zn ions are represented in gray color.

LTA4H is also a zinc metalloenzyme with dual catalytic functions, the activities of epoxide hydrolase and aminopeptidase.[99-101] As an epoxide hydrolase LTA4H is involved in arachidonic acid metabolism, it catalyses the hydrolysis of the epoxide LTA4 to the diol, leukotriene B4 (LTB4), which acts as chemoattractant and activator of inflammatory cells.[102-105] Therapeutic agents that selectively inhibit LTA4H can be potentially useful for the treatment of inflammation by blocking the formation of LTB4.[106]

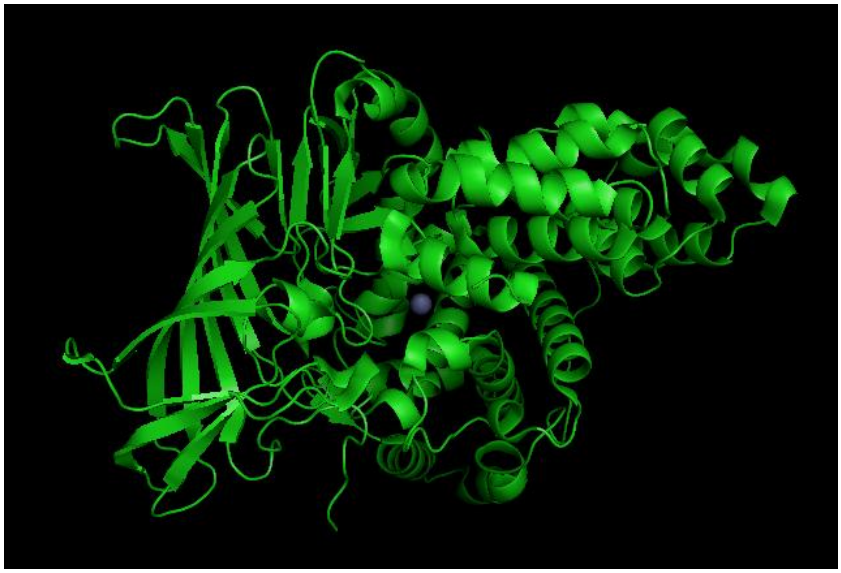

Figure III. 6. Crystal structure of Leukotriene A4 hydrolase (PDB 1HS6). LTA4H is a ~70 kDa zinc metalloenzyme. Catalytic zinc ion is shown in gray color.

In order to gain insights into the interactions between our photoprobe and its unexpected targets, we carried out blocking experiment using recombinant proteins. Photolabeling of recombinant Glo1 by our photoligand confirmed that this protein was indeed photolabeled directly by our photoprobe (Figure III.7.a). The calculated EC_{50}, that is the ligand concentration at which 50% of the maximum labeling is observed, was found to be 5 μM. Subsequently, the photolabeling experiment was repeated in the presence of excess adenine, benzophenone or biotin. As shown in Figure III.7.b, free benzophenone significantly reduced band intensity, whereas free adenine and biotin had no effect. This result indicated that Glo1 protein mainly recognized the benzophenone motif of our photoprobe. This is an important finding because Glo1 can come up as a background target in photoaffinity-labeling studies using benzophenone photoprobes.

Therefore, identification of benzophenone-recognizing proteins, such as Glo1, will be helpful for future studies.

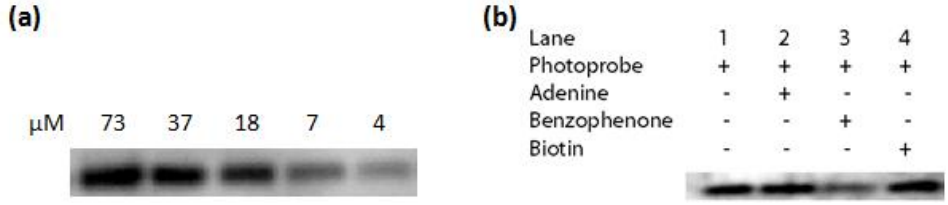

Figure III. 7. Photoaffinity labeling of recombinant Glo1. (a) Titration with different probe concentration. Based on the intensities of individual bands, EC_{50} (the ligand concentration at which 50% of the maximum labeling was observed) was calculated to be around 5 μM. (b) Blocking experiment with free adenine, benzophenone and biotin. As shown, benzophenone diminished the band intensity, whereas other blockers did not affect the intensity.

But Glo1 might not be just the background target of benzophenone photoaffinity-labeling. As mentioned earlier, benzophenone and similar frameworks are found in the structures of many clinical drugs, such as ketorpofen, suprofen and tiaprofenic acid (Figure III.8.a). The finding of Glo1 as a benzophenone-recognizing protein raised the possibility that Glo1 could be an off-target of such drugs. To test this hypothesis, we carried out the blocking experiment with ketoprofen. Ketoprofen is a nonsteroidal anti-inflammatory drug (NSAID) widely used for the treatment of arthritis and rheumatic diseases.[77] The therapeutic effects of ketoprofen are mediated by cyclooxygenases 1 and 2 (COX1 and COX2). As shown in Figure III.8.b ketoprofen significantly reduced the

band intensity. This indicates that Glo1 is a previously overlooked off-target of ketoprofen. The finding raises a new possibility that some of the beneficial as well as adverse effects of ketoprofen are mediated by Glo1.

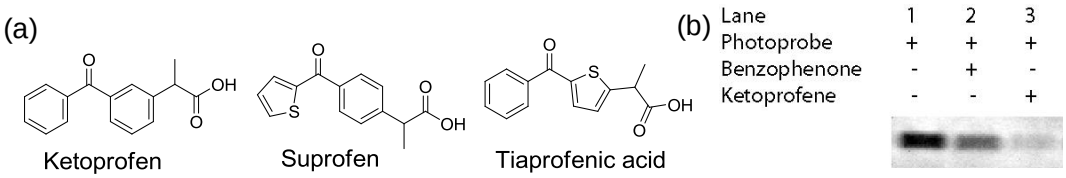

Figure III.8. (a) Structure of clinical drugs containing benzophenone or analogous frameworks. (b) Blocking experiment with benzophenone and ketoprofen. Ketoprofen significantly reduced the band intensity.

Photoaffinity-labeling and blocking experiments were also attempted with recombinant LTA4H, another "unexpected" target of adenine-benzophenone photoprobe. Despite our numerous attempts, however, recombinant LTA4H was not photolabeled by our photoprobe. There are several possible explanations. First, the purified recombinant LTA4H protein may behave differently from its native form in the cellular context where its biochemical properties are modulated by association with other proteins and/or post-translational modifications. Thus, it is possible that LTA4H is photolabeled only in the cellular context. Alternatively, LTA4H might have been photolabeled in cell lysates because it associates with the real target of our photoprobe and the LTA4H surface is within the reach of benzophenone. Another possibility is that LTA4H was not photolabeled but affinity purified because it binds to a photolabeled target protein. LTA4H is known to bind to actin related protein 2/3 complex subunit 3 (Y2H).[107]

The current study provided important clues to improve drug target identification using benzophenone photoligand. The study showed that blocking strategy can be used to classify potential targets identified from photoaffinity-labeling studies using benzophenone. Blocking study using recombinant proteins, however, is time consuming and also limited by the availability of recombinant proteins. A recombinant protein might behave differently from its native form in cell or tissue lysate. Blocking experiments, however, can be carried out using total cell lysates instead of recombinant proteins.[78] If blocking experiments using cell lysates are incorporated at the early stage of a study, it would eliminate the false positives and help the study focus on the real targets. This would facilitate the subsequent MS-based identification. Another challenge we encountered was the affinity purification of photolabeled proteins. As shown in Figure III.3, many photolabeled proteins were not affinity purified in our condition. The recovery of labeled proteins might be improved if photolabeled proteins are denatured prior to the affinity purification. Collectively, these challenges we encountered in the study led us to propose an improved procedure for drug target identification using benzophenone photoprobes (Scheme III.2).

1. Identification of drug targets using blocking strategy experiment

a) Cell Lysate
↓ BP – Drug
↓ hν
↓ SDS-PAGE
↓WESTERN

b) Cell Lysate
↓ BP – Drug + Free drug
↓ hν
↓ SDS-PAGE
↓WESTERN

2. Optimization of affinity purification method

a) Cell Lysate
↓ BP – Drug
↓ hν
↓ SDS-PAGE
↓WESTERN

b) Cell Lysate
↓ BP – Drug
↓ hν
↓ Affinity purification
↓ SDS-PAGE
↓WESTERN

c) Cell Lysate
↓ BP – Drug
↓ hν
↓ Denaturation
↓ Affinity Purification
↓ SDS-PAGE
↓WESTERN

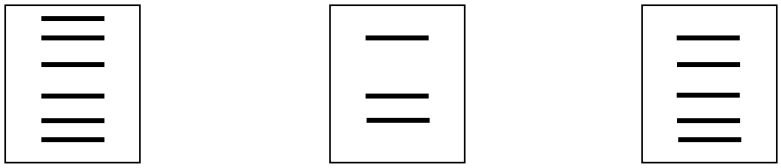

3. Large Scale Preparation

a) Cell Lysate
↓ BP – Drug
↓ hν
↓ Denaturation (if needed)
↓ Affinity purification
↓ SDS-PAGE
↓ Coomassie Staining

b) Cell Lysate
↓ BP – Drug + Free drug
↓ hν
↓ Denaturation (if needed)
↓ Affinity purification
↓ SDS-PAGE
↓ Coomassie Staining

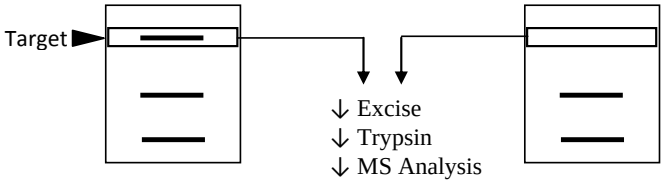

↓ Excise
↓ Trypsin
↓ MS Analysis

Scheme III.2 Proposed procedure for optimization of drug target identification using benzophenone photoprobes.*BP-benzophenone

III. 5 Experimental section

Materials

Fmoc-Gly-Wang resin, Fmoc-Gly, Fmoc-4-benzoyl-L-phenylaniline (Fmoc-L-Bpa), Fmoc-D-Bpa, dicyclohexylcarbodiimide (DCC), and 1-hydroxybenzotriazole (HOBt) were purchased from Fluka. Biotin-*N*-hydroxysuccinimide was obtained from Sigma-Aldrich. The Fmoc-protected peptide nucleic acid (PNA) adenine monomer, Fmoc-adenine-(Bhoc)-OH, was from Applied Biosystems. *N*-biotinyl-NH-$(PEG)_2$-COOH was available from Novabiochem, Switzerland (EMD Chemicals Catalog # 851029). Laemmli Sample Buffer, Tris-Glycine-SDS 10× buffer and Tris-Glycine 10× buffer were purchased from BioRad. Millipore Immobilon™ Western-chemiluminescent HRP (ECL) substrate was obtained through Fisher Scientific. Recombinant human Glyoxalase 1 was purchased from B&D Systems. Leukotriene A4 hydrolase (human recombinant) and ketoprofen from Cayman Chemical were obtained through Fisher Scientific. All other chemicals and solvents were obtained through Fisher Scientific and used without further purification.

Physico-Chemical analytical methods

Reversed phase (RP)-HPLC was performed on Agilent 1100 HPLC system equipped with 1100 Diode-Array Detector. Analytical RP-HPLC was performed using a Zorbax, Eclipse XDB-C8 (4.6 × 150mm) column (5 μm bead size). Semi-preparative HPLC was performed using Econosil C-18 10u (10 × 250 mm). Separation was achieved using a linear gradient at a flow rate of 1 ml/min (Analytical HPLC) or 3ml/min (Semi-

preperative HPLC) of Buffer **A** (20% ACN) and buffer **B** (100% ACN). Column effluent was monitored by UV absorbance at 254, 220, and 280 nm. Elution Conditions: t = 0 min A = 100%, t = 5 min A = 100%, t = 20 min A = 50%, t = 25 min A = 0, t = 30 min A = 100%.

Probes synthesis

The PEGylated adenine-benzophenone photoprobe was synthesized using SYMPHONY/Multiplex peptide synthesizer (RAININ-Instrument Co. Inc.) at Rockefeller University with the help of Dr. Mouli Chandramouli. SYMPHONY/Multiplex includes a vented solvent cabinet which is used for the storage of appropriate solvents. Up to six different solvents may be used automatically. Typically the primary solvent is DMF or NMP, deprotectant is piperidine/DMF solution. The activator solution is HBTU (*O*-Benzotriazole-*N,N,N',N'*-tetramethyl-uronium-hexafluoro-phosphate). When a coupling step is specified in the program, SYMPHONY/Multiplex automatically transfers the specified number of aliquots of the amino acid solution to the reaction vessel followed by the same volume of activator solution.

PEGylated adenine-benzophenone photoligand: **Biotinyl-polyethyleneglycol-p-benzoyl-L-phenylalanyl-glycinyl-N^9-acetyl-(2-aminoethyl)glycinyl-glycine**

Fmoc-Gly-Wang resin (200 mg, 0.15 mmol, loading of 0.75 mmol/gram, 1 eq.) was swollen in *N*-methyl-pyrolidone for 1 h at room temperature. The resin was washed 3

times with NMP. In order to remove the Fmoc group the resin was washed with a 20% piperidine in DMF solution for 10 min and again with the same solution for another 10 min. Next, the resin was washed 3 times with NMP, 5 min each. In the next step Fmoc-PNA-adenine(Bhoc) OH (151 mg, 0.30 mmol, 2 eq) was coupled to the resin using an equimolar HBTU activation. The Fmoc group was then removed and Fmoc-Gly-OH (90 mg, 0.30 mmol, 2 eq) was coupled using the same HBTU as a coupling reagent. Fmoc-L-Bpa (148 mg, 0.30 mmol, 2 eq) and *N*-biotinyl-NH-$(PEG)_2$-COOH (210 mg, 0.30 mmol, 2 eq) were coupled using the same HBTU methodology. The product was cleaved from the resin along with side chain deprotection by adding 10 ml of a 95% TFA, 2.5% TIS and 2.5% water solution. The mixture was allowed to stand for 2h, and then the volume TFA was reduced using N_2. The product was precipitated using cold petroleum ether. The total yield of the synthesis was 30%. The crude product was purified using semi-preparative HPLC, and relevant fractions were lyophilized to give a white solid. Analytical RP-HPLC retention time: 15.81 min. ESIMS (expected m/z 1201.4) m/z 1203.27 (MH^+). ^{1}H-NMR (500MHz, DMSO) 8.65 (1H, t, NH), 8.45 (1H, t, NH), 8.4 (1H, m, NH), 8.35 (1H, t, NH), 8.30 (1H, s, NH), 8.25 (1H, t, CH), 8.06 (1H, t, CH), 7.84 (1H, t, CH), 7.70-7.65 (9H, m, 9×CH), 7.57-7.37 (9H, m, 9×CH), 6.37 (2H, m, 2xNH), 5.30 (1H, s, CH), 5.20 (1H, s, CH), 4.30 (1H, m, CH), 4.13 (1H, m, CH), 4.03 (1H, s, CH), 3.88 (2H, d, CH_2), 3.84 (1H, m, CH), 3.80 (2H, m, CH_2), 3.76 (2H, m, CH_2), 3.65 (2H, m, CH_2), 3.50 (2H, m, CH_2), 3.45 (2H, m, CH_2), 3.37 (2H, m, CH_2), 3.23 (2H, m, CH_2), 3.15 (2H, m, CH_2), 3.06 (2H, m, CH_2), 2.85 (2H, m, CH_2), 2.05 (1H, t, OH), 1.93 (1H, t, CH), 1.76 (1H, s, CH), 1.60-1.43 (4H, m, 2xCH_2), 1.35-1.20 (6H, m, $CH_2CH_2CH_2$).

Cell culture and preparation of total lysate

THP1 cells were maintained in RPMI-1640 medium with 25 mM HEPES and L-Glutamine containing 10% fetal bovine serum (FBS), 1% penicillin-streptomycin amphotericin B (PSA) and 0.005μM β-mercaptoethanol, in a 37 ºC, 5% CO2 incubator. For each labeling experiment, cells were harvested at the log phase (50-70% confluency). Preparation of the cell lysate was carried out using M-Per® Mammalian Protein Extraction Reagent, which is formulated to retain the native structures of proteins. Cells were pelleted by centrifugation and then suspended in the M-Per® Reagent, 1ml reagent for ~100μL of wet cell pellet. Cell suspension was incubated at room temperature for 10 min, with gently shaking. The swelled cells were lysed by gentle pipetting. The lysates were centrifuged (10,000 rpm, 4 °C) and the supernatant (total lysate) was carefully transferred into a new Eppendorf tube on ice. Protein concentration was quantified with Promega Commassie Plus™ Protein Assay Reagent (Promega). Prior to photolabeling experiment, the final protein concentration was adjusted to 2 μg/μl with 1× TBS. The best result was obtained when protein solutions were kept on ice or in a refrigerator (4 °C) and used for photolabeling studies on the same day.

MCF7, HeLa, T24 and Calu1 cells, which are adherent cells, were maintained in RPMI-1640 medium with 25 mM HEPES and L-Glutamine containing 10% fetal bovine serum (FBS) and 1% penicillin-streptomycin amphotericin B (PSA), in a 37 ºC, 5% CO2 incubator. For each labeling experiment, cells were harvested at the log phase (50-70% confluency). Preparation of the cell lysate was carried out using M-Per® Mammalian Protein Extraction Reagent, which is formulated to retain the native structures of proteins. Briefly, the cell monolayer is rinse once with PBS (1×). Cells were directly lysed on the

tissue culture plate with 500µL of M-Per® Reagent. Cell lysate were scraped off from the plates and transferred into Eppendorfs tubes. The lysates were centrifuged (10,000 rpm, 4 °C) and the supernatant (total lysate) was carefully transferred into a new Eppendorf tube on ice. Protein concentration was quantified with Promega Commassie Plus™ Protein Assay Reagent (Promega). Prior to photolabeling experiment, the final protein concentration was adjusted to 2 µg/µl with Tris-buffered saline (TBS) (1×) The best result was obtained when protein solutions were kept on ice or in a refrigerator (4 °C) and used for photolabeling studies on the same day.

Photoaffinity purification, cell lines screening

40 µl aliquots of total lysate were mixed with 1 µl of a probe solution (3.67 mM in DMSO). Photocrosslinking was carried out under six Sylvania 350 Blacklight lamps (15 W, λmax 350 nm) for 1h, in which samples were kept on ice and placed approximately 5 cm below the lamps. ImmunoPure immobilized tetrameric Avidin was washed with TBS (1×) solution containing 1% Tween 20 (TBS-T) (1 minx5, 1000 rpm) and used for affinity purification. Following the photocrosslinking, sample was mixed with the avidin beads and incubated 30 min at 4 ºC. The supernatant was removed and the gel was vigorously washed with TBS (1×) solution containing 2% Tween 20. In the subsequent steps, protein solutions were always kept on ice or in a chromatography refrigerator (4 ºC). The sample was then mixed with Laemmli Sample Buffer (BioRad) 5%(v/v) 2- mercaptoethanol, denatured at 80 ºC for 5 min and separated on SDS-PAGE (10% Tris-HCl gel, 200 V, 1 h) in 1× Tris-Glycine-SDS buffer (BioRad). Gel was blotted onto PVDF membrane (200 mA, 2h) in a cold transfer buffer (20% methanol in 1×Tris-Glycine buffer). Blotted membrane was blocked with 5% non-fat milk in 50 mL TBS-T

for 1 h. Blocked membrane was rinsed with TBS-T (5 min), treated with avidin- hoarse radish peroxidase (HRP) (BioRad, 1:3000 dilution in 5% non-fat milk in TBS-T, 50 ml for 30 minutes), and washed with TBS-T (20 min×4). The washed membrane was treated with the Immobilon™ Western-chemiluminescent HRP substrate for 5 min. Bands were observed with the BioRad ChemiDoc gel documentation system.

Identification of cellular targets of PEGylated photoligand, affinity purification

6 ml of THP1 total lysate proteins (2 µg/µl) were mixed with 60 µl of PEGylated probe (3.7 mM in DMSO). Photocrosslinking was carried out under six Sylvania 350 Blacklight lamps (15 W, λ_{max} 350 nm) for 2 h, in which samples were kept on ice and placed approximately 5 cm below the lamps. ImmunoPure immobilized tetrameric Avidin was washed with TBS-T solution (1 minx5, 1000 rpm) and used for affinity purification. Following the photocrosslinking, sample was mixed with the avidin beads and incubated 30 min at 4 ºC. The supernatant was removed and the gel was vigorously washed with TBS (1×) solution containing 2% Tween 20. In the subsequent steps, protein solutions were always kept on ice or in a chromatography refrigerator (4 ºC). The sample was then mixed with Laemmli Sample Buffer (BioRad) 5%(v/v) 2- mercaptoethanol, denatured at 80 ºC for 5 min and separated on SDS-PAGE (5-20% Tris-HCl gel, 200 V, 1 h) in 1× Tris-Glycine-SDS buffer (BioRad). Gel was stained for 15 minutes with 0.5% Coomassie blue G-250 in a solution of 50% methanol/10% acetic acid. Stain was discarded and the gel was then destained with repeating washes with a solution of 40% methanol/10% acetic acid for 15-30 minutes until faint bands are observed. Gel was further destained using high purity water after which bands were excised and submitted for MS analysis.

Photolabeling of Glo1 and Western blot

30 µl aliquots of recombinant human Glo1 (0.05 µg/µl) are mixed with 3.7 mM photoprobe solution (Final probe dilutions are 1:50, 1:100, 1:200, 1:500 and 1:1000). For the blocking experiment the protein were mixed first with 20× blocking solution in DMSO (adenine, benzophenone, biotin and ketoprofen) and then with the probe solution in DMSO. The mixtures were incubated at 4 ºC for 1h. Photocrosslinking was carried out under six Sylvania 350 Blacklight lamps (15 W, λmax 350 nm) for 2 h, in which samples were kept on ice and placed approximately 5 cm below the lamps. Following the photocrosslinking, samples were mixed with Laemmli Sample Buffer (BioRad) with 5%(v/v) 2- mercaptoethanol, denatured at 80 ºC for 5 min and separated on SDS-PAGE (5-20% Tris-HCl gel, 200 V, 1 h) in 1× Tris-Glycine-SDS buffer (BioRad). Gel was blotted onto PVDF membrane (200 mA, 2h) in a cold transfer buffer (20% methanol in 1×Tris-Glycine buffer). Blotted membrane was blocked with 5% non-fat milk in Tris-buffered saline containing 1% Tween 20 (TBS-T) for 1 h. Blocked membrane was rinsed with TBS-T (5 min), treated with avidin- hoarse radish peroxidase (HRP) 17µL in 3% non-fat milk in TBS-T) for 30 minutes, and washed with TBS-T (20 min×3). The washed membrane was treated with the Immobilon™ Western-chemiluminescent HRP (ECL) reagent for 5 min. Bands were observed with the BioRad ChemiDoc gel documentation system.

Photolabeling of LTA4H and Western blot

Photolabeling of LTA4H and Western blot was conducted using the same procedure as described above for Glo1.

Chapter IV

Profiling of heat shock proteins with monomeric avidin

IV.1 Introduction

Heat shock proteins (Hsps) have long been considered as cytosolic proteins involved in the maintenance of protein folding.[108-111] When proteins are partially denatured in the cell, patches of hydrophobic surfaces are exposed and trigger protein aggregation, which can cause serious damages to the cell. Hsps bind to the exposed hydrophobic surfaces so as to prevent the aggregation and enable proteins to refold into their native structures.[112-114] A large number of Hsp homologs and isoforms, such as Hsp27s, Hsp40s, Hsp60s, Hsp70s, and Hsp90s, are known to exist and play vital roles in cell maintenance. This well-known group of "maintenance crews" in the cell, however, has recently been found in the extracellular milieus, such as cell surface and blood circulation.[48, 115-119] These circulating Hsps appear to be associated with various diseases including cancer and cardiovascular diseases.[46-52] However, minuscule quantities of circulating Hsps make it difficult to identify and characterize circulating Hsp species in a reproducible manner.

The most widely used method for studying circulating Hsps is enzyme-linked immunosorbent assay (ELISA). However, several weaknesses have been recognized for this method. Its performance largely depends on the quality of antibody as well as operator skills and experience. Also the method is limited by its ability to measure only a single protein at a time in a given sample aliquot.[120, 121] Another potential shortcoming of ELISA is that the method depends on the availability of antibodies: There is no guarantee that high quality antibodies are available for all different variants of the protein of interest, such as polymorphism and posttranslational modifications. For example, Hsp 90 is one of the major phosphorylated proteins found in cells.[122-124] While

phosphorylation of Hsp90 is relatively slow at 37 °C, the rate rapidly increases at heat shock temperatures.[125, 126] Another posttranslational modification that has been reported for Hsp70 and Hsp90 is acetylation.[127, 128] ELISA cannot be used to probe many of these post-translationally modified proteins because of the lack of suitable antibodies. One powerful approach that can complement the shortcomings of ELISA is proteomic profiling based on mass spectrometry (MS). However, direct MS analysis of minute serum proteins is difficult because predominant serum proteins, such as albumin and immunoglobulins, would mask the signals of minor constituents. In order to analyze Hsps in serum by MS, therefore, it is necessary to either remove the predominant proteins or selectively enrich Hsps from serum sample.

A simple chemical approach to selectively enrich Hsps from complex proteomes, such as cell lysates and serum samples is presented in this chapter. This approach is based on our serendipitous finding that monomeric avidin, which is a commercially available avidin resin for affinity purification, binds selectively to a variety of Hsp species in cell lysates. Monomeric and tetrameric avidin affinity columns are widely used in biological systems for purification and detection of various biomolecules.[129-131] Avidin is a homotetramer with a high degree of affinity and specificity to biotin ($K_d = 10^{-15}$ M).[79, 81] The non-reversible nature of the tetrameric avidin-biotin complex can be a problem when release of the captured ligand is desirable without using harsh denaturing conditions. Monomeric avidin resin, which is obtained by partially denaturing tetrameric avidin on agarose, has a reduced affinity for biotin ($K_d = 10^{-7}$ M) and is widely used in applications that require capture and release biotinylated proteins under mild conditions.[129, 132-134] As presented in this chapter, however, our recent study revealed that monomeric avidin is

also able to enrich Hsps from complex proteomes in a reproducible manner. Monomeric avidin, therefore, can serve as a simple and powerful tool to reproducibly analyze circulating Hsps to define their potential roles in various diseases.

IV.2 Discovery of monomeric avidin as a new tool for the enrichment of Hsps from complex proteomes

The ability of monomeric avidin to enrich Hsps was discovered when we were conducting affinity purification of photochemically biotinylated proteins from a cytosolic lysate of Jurkat cells, a cell line derived from human T-cell leukemia.[82] During this study, background protein-binding to monomeric avidin was assessed with Jurkat lysate without chemically biotinylated proteins (negative control). Jurkat lysate was incubated with monomeric avidin resin and washed with Tris-buffered saline (TBS) buffer containing 0.1% Tween, which removed non-specifically bound proteins on the surface of monomeric avidin. When background proteins were resolved by SDS-PAGE and visualized by Coomassie blue staining, it was found that monomeric avidin resin gave background Coomassie-stained bands distinctly different from Jurkat cytosol bands (Figure IV.1, lane 2). Tetrameric avidin resin, on the other hand, did not give any visible background bands (Figure IV.1, lane 3). The proteins bound to the monomeric avidin resin did not appear to be non-specific bindings of abundant proteins, because many of the strongest bands in the original lysate were not observed in the proteins enriched by monomeric avidin. Instead, the distinct profile suggested some specific enrichment of certain proteins by monomeric avidin. We, therefore, decided to conduct the identification of those enriched proteins by mass spectrometry. Mass spectrometric

analyses revealed that the distinct Coomassie-stained bands contained 14 different Hsps, namely four chaperonin containing TCP1 isoforms (Hsp60s), six Hsp70 isoforms, and four Hsp90 isoforms (Table IV.1). A complete list of proteins enriched by monomeric avidin is shown in Appendix 2.

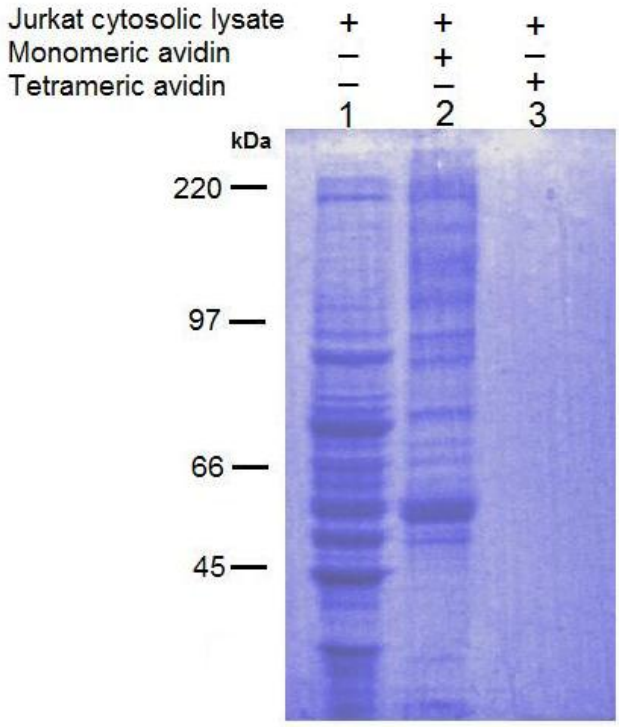

Figure IV.1. Avidin affinity purification of Jurkat cytosolic lysate. Jurkat cytosolic lysate (2µg/µL) was incubated with monomeric and tetrameric avidin respectively, separated by SDS-PAGE and visualized by Coomassie staining. Lane 1: Jurkat cytosolic lysate; lane 2: Jurkat cytosolic lysate after avidin affinity purification using monomeric avidin; lane 3: Jurkat cytosolic lysate after avidin affinity purification using tetrameric avidin.

Table IV.1. Jurkat cytosolic proteins enriched monomeric avidin affinity resin.

Band	Gene identifier	Mass	Gene
220	12667788	227646	myosin, heavy polypeptide 9, non-muscle [135]
90	306891	83584	**90kDa heat shock protein**
90	4503483	96246	eukaryotic translation elongation factor 2 [Homo sapiens]
90	15010550	90309	**heat shock protein gp96 precursor [Homo sapiens]**
90	67477458	80345	**heat shock protein 75kDa, mitochondrial precursor [Homo sapiens]**
90	83699649	98652	**heat shock 90 kDa protein 1, alpha [Homo sapiens]**
70	3522	71209	**heat shock 70kDa protein 6 (HSP70B') [Homo sapiens]**
70	188488	70294	**heat shock-induces protein**
70	4204880	70237	**heat shock protein [Homo sapiens]**
70	4504965	70851	L-plastin [Homo sapiens]
70	4505257	67892	moesin [Homo sapiens]
70	5729877	71082	**heat shock 70kDa protein 8 isoform 1 [Homo sapiens]**
70	21753703	75551	WD repeat domain 67 [Homo sapiens]
70	21759781	70748	**heat shock 70kDa protein 1-like [Homo sapiens]**
70	62089222	78018	**heat shock 70kDa protein 1A variant [Homo sapiens]**
60	35505	58411	pyruvate kinase [Homo sapiens]
60	189238	63377	neuroleukin
60	1136741	59035	**chaperonin containing TCP1, subunit 8 (theta) [Homo sapiens]**
60	4502643	58444	**chaperonin containing TCP1, subunit 6A isoform a [Homo sapiens]**
60	5453607	59842	**chaperonin containing TCP1, subunit 7 isoform a [Homo sapiens]**
60	1200184	58316	**chaperonin containing TCP1, subunit 4 (delta) [Homo sapiens]**
50	223486	49830	tubulin beta
50	1002923	51722	coronin, actin binding protein, 1A [Homo sapiens]
50	4507729	50274	tubulin, beta 2 [Homo sapiens]
50	9507215	50746	tubulin, alpha 8 [Homo sapiens]
50	14389309	50548	tubulin, alpha 6 [Homo sapiens]
50	57209813	48135	tubulin beta polypeptide [Homo sapiens]
45	927065	43139	eukaryotic translation elongation factor 1 alpha 1-like 14 [Homo sapiens]
45	109071712	48181	eukaryotic translation elongation factor 1 alpha 1 [Homo sapiens]
45	4503571	47481	enolase 1 [Homo sapiens]
45	4503573	47271	enolase 3 [Homo sapiens]
45	5803011	47581	enolase 2 [Homo sapiens]

IV.3 Reproducible enrichment of Hsps from serum samples with monomeric avidin

The observed selectivity of monomeric avidin towards Hsps opened the possibility that monomeric avidin resin might serve as a general tool to enrich circulating Hsps, which, as mentioned earlier, are difficult to analyze due to their minute quantities in blood circulation. To test this, human serum samples from donors with and without colorectal cancer were incubated with monomeric avidin resin. This time, samples were washed under more stringent conditions (ten times with TBS containing 2% Tween) to completely remove weakly bound proteins. Tightly bound proteins were then separated by SDS-PAGE and visualized with Coomassie blue stain (Figure IV.2.a). This analysis reproducibly showed a number of distinct Coomassie stained bands in the serum of the donor with colorectal cancer but not in the control sample. We also compared the blood serum profiles by using silver staining, which is one to two orders of magnitudes more sensitive than Coomassie stain,[136, 137] to visualize bands that are overlooked in the Coomassie stain. The silver staining suggested that the difference between the two samples might be smaller than Coomassie staining. However, there were a few notable differences, such as the band around 60 kDa (Figure IV.2 b).

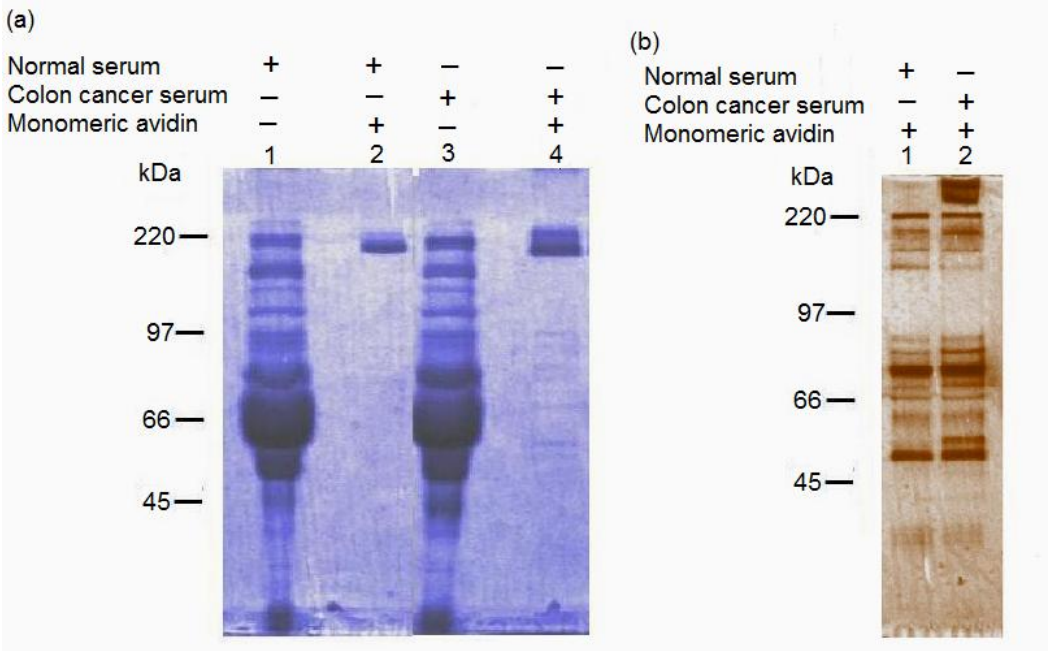

Figure IV.2. Affinity purification of serum samples using monomeric avidin. Serum samples from a healthy donor and a donor with colon cancer (2 µg/µL) were incubated with monomeric avidin, separated by SDS-PAGE and visualized by (a) Coomassie staining and (b) silver staining. (a) Lane 1: normal serum; lane 2: normal serum proteins enriched by monomeric avidin; lane 3: colon cancer serum; lane 4: colon cancer serum proteins enriched by monomeric avidin. (b) Lane 1: normal serum proteins enriched by monomeric avidin; lane 2: colon cancer serum proteins enriched by monomeric avidin. Triplicate experiments were conducted and a representative gel image is shown.

Since one of the most distinctively different bands between the two samples was around 60 kDa, the expression levels of Hsp60 in these samples were analyzed with Western blot with anti-human Hsp60 antibody (Figure IV.3). The analysis revealed that one of the enriched proteins was indeed Hsp60 and its level was consistently higher ($p < 0.05$) in the sample from the donor with colorectal cancer than in the control. Although

further studies are needed to examine the correlation between extracellular Hsp60 and colon cancer, our current study suggests that monomeric avidin can be employed to reproducibly enrich extracellular Hsps from serum samples.

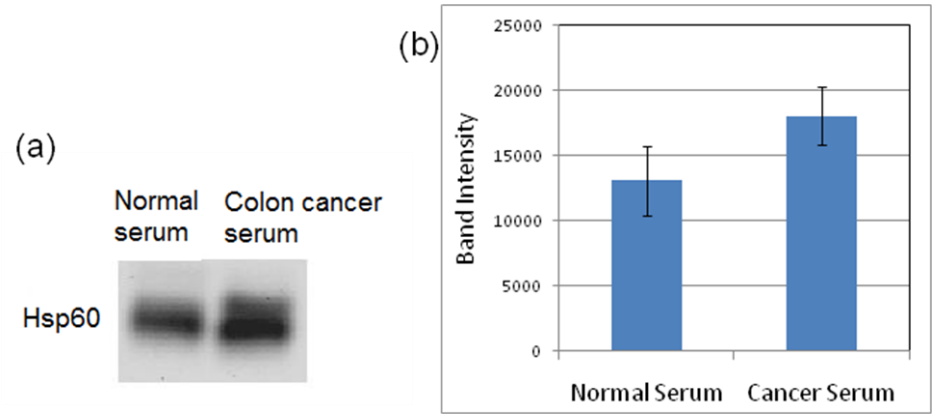

Figure IV.3. Expression levels of Hsp60 in serum samples using anti-human Hsp60 antibody. (a) Western blot of serum samples. (b) Quantification of the labeling signals for normal and cancer serum samples. Results are the average values ± standard errors for four independent experiments ($p < 0.05$).

IV.4 Discussion

Enrichment of low-abundance proteins is becoming an increasingly important concept in proteomic research because the presence of abundant proteins, such as albumin and immunoglobulin, obscure the analyses of low abundance proteins.[138-141] Although there are a number of commercial kits that deplete 80-95% of albumin and immunoglobulin, the large dynamic range of serum protein concentration (i.e., 10 orders

of magnitude or higher)[138] suggests that many low abundance proteins can still be obscured by the residual albumin and immunoglobulin.

Several new technologies have been developed recently for the enrichment and detection of low-abundance proteins in complex proteomes. For example, one approach uses peptide library beads, in which immobilized peptide ligands are used to enrich their target proteins. In this way, the method successfully reduces the concentration of most abundant proteins, while simultaneously enhancing the concentration of low abundance proteins.[135, 142-144] In a similar approach Kodadek *et al*. used peptoid library beads to enrich ligand proteins in complex proteomes. Peptoids, which are peptide analogous with the side chain attached to amino nitrogens rather than the alpha-carbons, exhibit similar binding characteristics as peptide ligands. The advantage of peoptoids over peptides, however, is that peptoids are not susceptible to cleavage by proteases which exist in cell and tissue samples and can degrade the peptide ligands and alter their binding characteristic.[145-149]

The monomeric avidin method, which was discovered in our study, is conceptually similar to peptide and peptoid bead approaches. The mechanism of selective Hsp enrichment can be understood when we consider how monomeric avidin is prepared. Preparation of monomeric avidin is a multistep denaturation-renaturation procedure. First tetrameric streptavidin is immobilized to cyanogen bromide-activated agarose. Second, immobilized tetrameric avidin is subjected to chemical denaturation, in which avidin proteins dissociate into individual monomers. Any non-immobilized subunits are removed from the resin at this stage. Finally, the immobilized avidin subunits are renatured to generate the monomeric avidin matrix. The monomers are partially

denatured proteins with lower affinity to biotin, but the diminished affinity to biotin make it suitable for certain affinity chromatography applications.[129, 132, 134] The selective binding of Hsps to monomeric avidin can be explained based on the partially denatured structure of monomeric avidin on the solid resin. Immobilized avidin monomers expose various partially unfolded hydrophobic peptides which serve as recognition motifs for Hsps (Figure IV.4). The chemical denaturation of tetrameric avidin, followed by renaturation of immobilized avidins, however, is not a uniform process. Thus, the process of monomeric avidin production inadvertently creates various hydrophobic motifs that can serve as baits for Hsps.

Importantly, the development of simple and reproducible method for Hsp enrichment opens a new opportunity to define the roles of circulating Hsps in various diseases. As mentioned in the Introduction section, circulating Hsps have been associated with cancer, and cardiovascular diseases. [46-52] Our preliminary study indeed indicates that Hsp60 level might correlate with colon cancer, although much more comprehensive studies are needed to test this hypothesis.

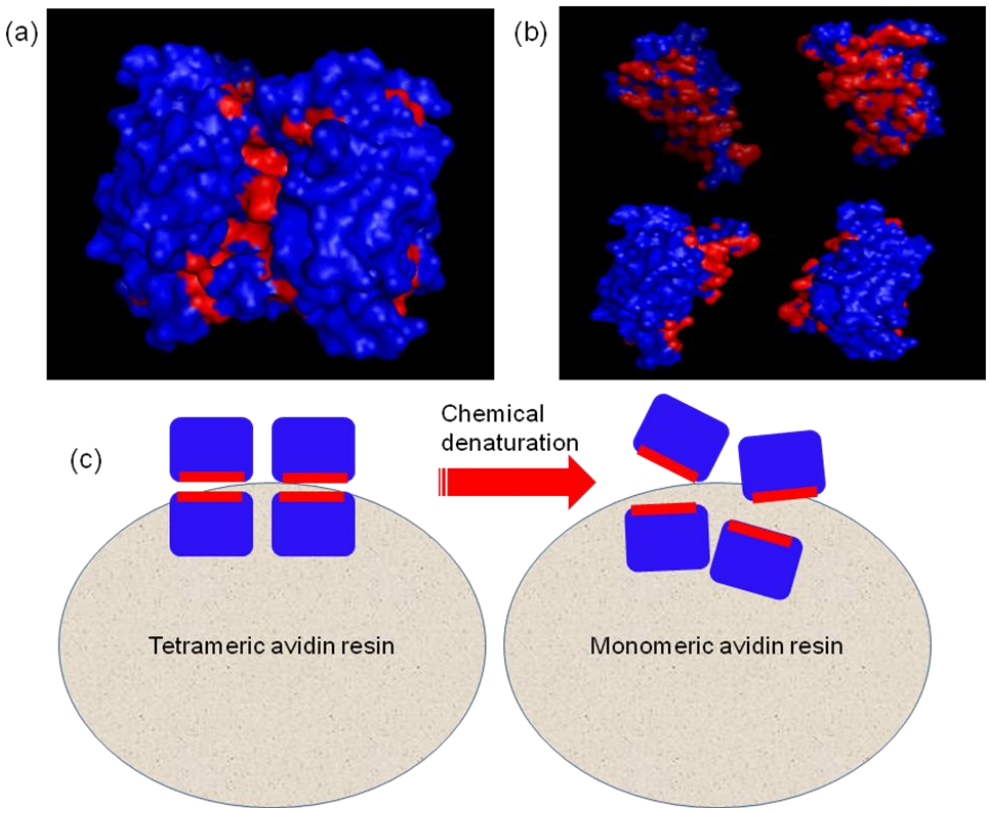

Figure IV.4. Breakage of tetrameric avidin results in the exposure of interior surfaces. (a) Tetrameric streptavidin (PDB 3MG5). Avidin-avidin interfaces, which are mostly composed of hydrophobic residues, are shown in red, whereas hydrophilic surfaces are shown in blue. (b) Monomeric avidin exposes the internal hydrophobic surfaces which serve as the baits for Hsps. (c) Schematic diagram of chemical denaturation of tetrameric avidin, which results in the exposure of hydrophobic surfaces.

There is a clear and urgent need for new serum biomarkers of cancer and other serious diseases. Most of the existing serum biomarkers suffer from poor specificity and sensitivity.[150] For example, cancer antigen 125 (CA125) is the most widely used biomarker for ovarian cancer but it detects only 50% of the early stage ovarian cancer.[151,

[152] The prostate-specific antigen (PSA) test is used in prostate cancer screening. However, the test can not differentiate between early stages and the more aggressive cancers.[150, 153] The monomeric avidin method presented in this chapter provides a unique opportunity to characterize the distribution and abundance of circulating Hsps in a quantitative manner, which may result in the discovery of new diagnostic and prognostic biomarkers of various diseases.

IV. 4 Experimental section

Materials

Laemmli Sample Buffer, Tris-Glycine-SDS 10× buffer, Tris-Glycine 10× buffer and Criterion Tris-HCl Gel, 10% polyacrylamide gel, 12+2 well, 45 μl, 13.3 × 8.7 cm were purchased from BioRad. Immobilon™ Western-chemiluminescent HRP substrate and Millipore Immobilon-P polyvinylidene fluoride (PVDF) membrane were obtained from Millipore. Pierce® Avidin Agarose and Pierce® Monomeric Avidin Agarose were purchased through Fisher Scientific. Blood serum samples were obtained from Asterand, XpressBANK. Purified Mouse-Anti-Hsp60 was purchased from BD Biosciences. All other chemicals and solvents were obtained through Fisher Scientific and used without further purification.

Cell culture and lysate preparation

Jurkat cells were maintained in RPMI-1640 medium with 25 mM HEPES and L-Glutamine containing 10% fetal bovine serum (FBS) and 1% penicillin-streptomycin amphotericin B (PSA), in a 37 ºC, 5% CO_2 incubator. For each labeling experiment, cells were harvested at the log phase (50-70% confluency). To obtain the cytosolic lysates of Jurkat cells, cells were pelleted by centrifugation and then suspended in the 1× hypotonic lysing buffer (pH 7.3, 10 mM HEPES, 1.5 mM $MgCl_2$, 10 mM KCl, 0.1mM EDTA, and 1 mM phenylmethanesulfonylfluoride (PMSF)) (1 mL). Cell suspension was incubated at room temperature for 10 min. The swelled cells were lysed by gentle pipetting. The lysates were centrifuged (10,000 rpm, 4 °C) and the supernatant (cytosolic lysate) was

carefully transferred into a new Eppendorf tube on ice. Protein concentration is quantified with Promega Commassie Plus™ Protein Assay Reagent (Promega). The final protein concentration was adjusted to 2 µg/µl with 1× TBS. The best result was obtained when protein solutions were kept on ice or in a refrigerator (4 °C) and used for photolabeling studies on the same day.

Identification of cellular targets, avidin affinity purification

Avidin and monomeric avidin beads were washed with TBS (1×) solution containing 0.1% Tween 20 (TBS-T) solution (1 min×5, 1000 rpm) and used for affinity purification. 3 ml of Jurkat cytosolic lysate proteins (2 µg/µl) were mixed with 150 µl avidin and monomeric avidin, respectively, and incubated for 2 hours at 4 ºC. The supernatant was removed and the gel was vigorously washed with TBS-T. In the subsequent steps, protein solutions were always kept on ice or in a chromatography refrigerator (4 ºC). The sample was then mixed with Laemmli Sample Buffer (BioRad) 5%(v/v) 2- mercaptoethanol, denatured at 80 ºC for 5 min and separated on SDS-PAGE (5-20% Tris-HCl gel, 200 V, 1 h) in 1× Tris-Glycine-SDS buffer (BioRad). Gel was stained for 15 minutes with 0.5% Coomassie blue G-250 in a solution of 50% methanol/10% acetic acid. Stain was discarded and the gel was then destained with repeating washes with a solution of 40% methanol/10% acetic acid for 15-30 minutes until faint bands are observed. Gel was further destained using high purity water after which bands were excised and submitted for MS analysis.

Coomassie staining of human serum sample

Human serum samples from donors with (D1) and without colorectal cancer (A3) were incubated with monomeric avidin resin. Serum concentration was quantified with Promega Commassie Plus™ Protein Assay Reagent (Promega). The final serum concentration was adjusted to 2 µg/µl with 1× TBS. Monomeric avidin beads were washed with TBS-T solution (1 min×5, 1000 rpm) and used for affinity purification. 2 ml of serum samples (2 µg/µl) were mixed with 150 µl monomeric avidin resin and incubated for 2 hours at 4 ºC. The supernatant was removed and the gel was vigorously washed with TBS (1×) solution containing 2% Tween 20. In the subsequent steps, serum solutions were always kept on ice or in a chromatography refrigerator (4 ºC). The sample was then mixed with Laemmli Sample Buffer (BioRad) 5%(v/v) 2- mercaptoethanol, denatured at 80 ºC for 5 min and separated on SDS-PAGE (5-20% Tris-HCl gel, 200 V, 1 h) in 1× Tris-Glycine-SDS buffer (BioRad). Gel was stained for 15 minutes with 0.5% Coomassie blue G-250 in a solution of 50% methanol/10% acetic acid. Stain was discarded and the gel was then destained with repeating washes with a solution of 40% methanol/10% acetic acid for 15-30 minutes until faint bands are observed. Gel was further destained using high purity water.

Silver staining of human serum sample

Human serum samples from donors with (D1) and without colorectal cancer (A3) were incubated with monomeric avidin resin. Serum concentration was quantified with Promega Commassie Plus™ Protein Assay Reagent (Promega). The final serum concentration was adjusted to 2 µg/µl with 1× TBS. Monomeric avidin beads were

washed with TBS-T solution (1 min×5, 1000 rpm) and used for affinity purification. 2 ml of serum samples (2 µg/µl) were mixed with 150 µl monomeric avidin resin and incubated for 2 hours at 4 ºC. The supernatant was removed and the gel was vigorously washed with TBS (1×) solution containing 2% Tween 20. In the subsequent steps, serum solutions were always kept on ice or in a chromatography refrigerator (4 ºC). The sample was then mixed with Laemmli Sample Buffer (BioRad) 5%(v/v) 2- mercaptoethanol, denatured at 80 ºC for 5 min and separated on SDS-PAGE (5-20% Tris-HCl gel, 200 V, 1 h) in 1× Tris-Glycine-SDS buffer (BioRad). Gel was fixed in 150 ml solution of 50% methanol/45% distilled water/5% acetic acid for 20 minutes and washed in 150 ml 50% methanol aq. for 10 minutes followed by washing in 150 ml distilled water for another 10 minutes. The gel was sensitized in 150 ml 0.02% sodium thiosulfate for 1 minute and rinsed with 150 ml distilled water (1 minute ×2). The sensitized gel was submerged in 150 ml 0.1% silver nitrate with 0.08% formaldehyde for 20 minutes and rinsed with distilled water (1 minute ×2). A fresh developing solution must be prepared every time just before adding. The gel was incubated with 150 ml 2% sodium carbonate containing 0.04% formaldehyde until the desired intensity of staining occurs. If developer turns yellow within 30 seconds, discard and replace with fresh 150 ml developer. Developing reaction was stopped by adding 150 ml 5% acetic acid for 10 minutes.

Western blot of human serum sample

Human serum samples from donors with (D1) and without colorectal cancer (A3) were incubated with monomeric avidin resin. Serum concentration was quantified with Promega Commassie Plus™ Protein Assay Reagent (Promega). The final serum concentration was adjusted to 2 µg/µl with 1× TBS. Monomeric avidin beads were

washed with TBS-T solution (1 min×5, 1000 rpm) and used for affinity purification. 250 µl of serum samples (2 µg/µl) were mixed with 50 µl monomeric avidin resin and incubated for 2 hours at 4 ºC. The supernatant was removed and the gel was vigorously washed with TBS (1×) solution containing 2% Tween 20. In the subsequent steps, serum solutions were always kept on ice or in a chromatography refrigerator (4 ºC). The sample was then mixed with Laemmli Sample Buffer (BioRad) 5%(v/v) 2- mercaptoethanol, denatured at 80 ºC for 5 min and separated on SDS-PAGE (5-20% Tris-HCl gel, 200 V, 1 h) in 1× Tris-Glycine-SDS buffer (BioRad). Gel was blotted onto PVDF membrane (200 mA, 2h) in a cold transfer buffer (20% methanol in 1×Tris-Glycine buffer). Blotted membrane was blocked with 5% non-fat milk in 50 mL TBS-T for 1 h. Blocked membrane was rinsed with TBS-T (5 min) and incubated overnight with primary antibody (mouse anti-Hsps60) (1:5000 dilution in 3% non-fat milk in TBS-T 5ml). After primary antibody incubation the membrane was washed with TBS-T for 10 min. The washed membrane was incubated 1h with secondary antibody (goat anti-mouse IgG HRP conjugate) (1:5000 dilution in 5% non-fat milk in TBS-T 10 ml). The membrane was washed with TBS-T (20 min×3). The washed membrane was treated with the Immobilon™ Western-chemiluminescent HRP substrate for 5 min. Bands were observed with the BioRad ChemiDoc gel documentation system.

Appendix 1

GI	Name	Mass	Score
gi|51247429	Chain A, Structure Of [r563a] Leukotriene A4 Hydrolase	69652	893
gi|2392338	Chain A, Human Glyoxalase I With Benzyl-Glutathione Inhibitor	20861	198
gi|28592	serum albumin [Homo sapiens]	71316	175
gi|28317	unnamed protein product [Homo sapiens]	59720	128
gi|62897409	beta actin variant [Homo sapiens]	42038	100
gi|16359158	Actin, beta [Homo sapiens]	42078	80
gi|160013026	ANKRD26-like family C member 1B (Chimeric POTE-actin protein)	122946	80
gi|134133226	protein expressed in prostate, ovary, testis, and placenta 2 [Homo sapiens]	122882	80
gi|3891517	Chain A, Human Glyoxalase I Q33e, E172q Double Mutant	20861	75
gi|4501881	alpha 1 actin precursor [Homo sapiens]	42366	73
gi|4501883	alpha 2 actin [Homo sapiens]	42381	73
gi|553734	putative [Homo sapiens]	2269	69
gi|62896585	adenylyl cyclase-associated protein variant [Homo sapiens]	51899	62
gi|16751921	dermcidin preproprotein [Homo sapiens]	11391	56
gi|148271063	dermcidin isoform 2 [Homo sapiens]	12520	56
gi|12276066	3-methylcrotonyl-CoA carboxylase alpha subunit [Homo sapiens]	80895	55
gi|51476873	hypothetical protein [Homo sapiens]	64269	55
gi|62898171	L-plastin variant [Homo sapiens]	70785	52
gi|46411195	PIG48 [Homo sapiens]	61110	50
gi|671527	gamma subunit of CCT chaperonin [Homo sapiens]	60862	50
gi|34526448	unnamed protein product [Homo sapiens]	53733	46
gi|16040977	Rb1-inducible coiled coil protein [Homo sapiens]	185051	38
gi|30293	unnamed protein product [Homo sapiens]	67347	38
gi|119575046	hCG2025155 [Homo sapiens]	9767	37
gi|51316478	GTP-binding protein REM 2 (Rad and Gem-like GTP-binding protein 2)	36170	37
gi|4506675	ribophorin I precursor [Homo sapiens]	68641	36
gi|119581184	ATP citrate lyase, isoform CRA_c [Homo sapiens]	69678	35
gi|38569423	ATP citrate lyase isoform 2 [Homo sapiens]	120608	35
gi|68533125	ACLY variant protein [Homo sapiens]	125389	35
gi|28935	ATP-citrate (pro-S-)-lyase [Homo sapiens]	122197	35
gi|703118	thyroid receptor interactor	35892	35
gi|119590696	membrane protein, palmitoylated 4 (MAGUK p55 subfamily member 4), isoform CRA_f [Homo sapiens]	51236	34
gi|34529517	unnamed protein product [Homo sapiens]	21366	34

gi|11139299	membrane-spanning 4-domains, subfamily A, member 7 isoform 1 [Homo sapiens]	26399	34
gi|37492	alpha-tubulin [Homo sapiens]	50810	34
gi|340021	alpha-tubulin	50804	34
gi|14389309	tubulin alpha 6 [Homo sapiens]	50548	34
gi|119600189	ribosomal protein L24, isoform CRA_d [Homo sapiens]	19569	34
gi|55960095	dystonin [Homo sapiens]	861913	34
gi|18157651	bullous pemphigoid antigen 1 eA [Homo sapiens]	593646	34
gi|34577047	dystonin isoform 1 [Homo sapiens]	632532	34
gi|169163653	PREDICTED: hypothetical protein [Homo sapiens]	N/A	34
gi|49227854	mediator complex subunit 10 [Homo sapiens]	N/A	33
gi|112181294	ELMO/CED-12 domain containing 1 [Homo sapiens]	N/A	33
gi|51247429	Chain A, Structure Of [r563a] Leukotriene A4 Hydrolase	69652	893
gi|2392338	Chain A, Human Glyoxalase I With Benzyl-Glutathione Inhibitor	20861	198
gi|28592	serum albumin [Homo sapiens]	71316	175
gi|28317	unnamed protein product [Homo sapiens]	59720	128
gi|62897409	beta actin variant [Homo sapiens]	42038	100
gi|16359158	Actin, beta [Homo sapiens]	42078	80
gi|160013026	ANKRD26-like family C member 1B (Chimeric POTE-actin protein)	122946	80
gi|134133226	protein expressed in prostate, ovary, testis, and placenta 2 [Homo sapiens]	122882	80
gi|3891517	Chain A, Human Glyoxalase I Q33e, E172q Double Mutant	20861	75
gi|4501881	alpha 1 actin precursor [Homo sapiens]	42366	73
gi|4501883	alpha 2 actin [Homo sapiens]	42381	73
gi|553734	putative [Homo sapiens]	2269	69
gi|62896585	adenylyl cyclase-associated protein variant [Homo sapiens]	51899	62
gi|16751921	dermcidin preproprotein [Homo sapiens]	11391	56
gi|148271063	dermcidin isoform 2 [Homo sapiens]	12520	56
gi|12276066	3-methylcrotonyl-CoA carboxylase alpha subunit [Homo sapiens]	80895	55
gi|51476873	hypothetical protein [Homo sapiens]	64269	55
gi|62898171	L-plastin variant [Homo sapiens]	70785	52
gi|46411195	PIG48 [Homo sapiens]	61110	50
gi|671527	gamma subunit of CCT chaperonin [Homo sapiens]	60862	50
gi|34526448	unnamed protein product [Homo sapiens]	53733	46
gi|16040977	Rb1-inducible coiled coil protein [Homo sapiens]	185051	38
gi|30293	unnamed protein product [Homo sapiens]	67347	38
gi|119575046	hCG2025155 [Homo sapiens]	9767	37
gi|51316478	GTP-binding protein REM 2 (Rad and Gem-like GTP-binding protein 2)	36170	37

gi|4506675	ribophorin I precursor [Homo sapiens]	68641	36
gi|119581184	ATP citrate lyase, isoform CRA_c [Homo sapiens]	69678	35
gi|38569423	ATP citrate lyase isoform 2 [Homo sapiens]	120608	35
gi|68533125	ACLY variant protein [Homo sapiens]	125389	35
gi|28935	ATP-citrate (pro-S-)-lyase [Homo sapiens]	122197	35
gi|703118	thyroid receptor interactor	35892	35
gi|119590696	membrane protein, palmitoylated 4 (MAGUK p55 subfamily member 4), isoform CRA_f [Homo sapiens]	51236	34
gi|34529517	unnamed protein product [Homo sapiens]	21366	34
gi|11139299	membrane-spanning 4-domains, subfamily A, member 7 isoform 1 [Homo sapiens]	26399	34
gi|37492	alpha-tubulin [Homo sapiens]	50810	34
gi|340021	alpha-tubulin	50804	34
gi|14389309	tubulin alpha 6 [Homo sapiens]	50548	34
gi|119600189	ribosomal protein L24, isoform CRA_d [Homo sapiens]	19569	34
gi|55960095	dystonin [Homo sapiens]	861913	34
gi|18157651	bullous pemphigoid antigen 1 eA [Homo sapiens]	593646	34
gi|34577047	dystonin isoform 1 [Homo sapiens]	632532	34
gi|169163653	PREDICTED: hypothetical protein [Homo sapiens]	N/A	34
gi|49227854	mediator complex subunit 10 [Homo sapiens]	N/A	33
gi|112181294	ELMO/CED-12 domain containing 1 [Homo sapiens]	N/A	33
gi|4689262	sorting nexin 11 [Homo sapiens]	N/A	33
gi|119607690	hCG1642689, isoform CRA_a [Homo sapiens]	N/A	33
gi|32479364	outer dense fiber of sperm tails 2 isoform 3 [Homo sapiens]	76140	33
gi|119568930	MDN1, midasin homolog (yeast), isoform CRA_a [Homo sapiens]	638034	32
gi|10434275	unnamed protein product [Homo sapiens]	64050	32
gi|159162689	Chain A, Human Protein Disulfide Isomerase, Nmr, 40 Structures	13363	32
gi|183769	3-alkyladenine DNA glycosylase	33268	32
gi|4503031	CASP2 and RIPK1 domain containing adaptor with death domain [Homo sapiens]	22788	31
gi|119631362	NCK-associated protein 1, isoform CRA_f [Homo sapiens]	43731	31
gi|119607257	hCG1988300, isoform CRA_b [Homo sapiens]	47891	31
gi|119591067	hCG15580 [Homo sapiens]	17550	31
gi|4503979	glial fibrillary acidic protein [Homo sapiens]	49907	31
gi|119567960	hCG1643231, isoform CRA_a [Homo sapiens]	19005	31
gi|31873640	hypothetical protein [Homo sapiens]	54655	31
gi|34526058	unnamed protein product [Homo sapiens]	13550	31
gi|168985723	major histocompatibility complex, class I, B [Homo sapiens]	27831	31
gi|12667788	myosin, heavy polypeptide 9, non-muscle [Homo	227646	31

	sapiens]		
gi|119592244	myosin, heavy polypeptide 14, isoform CRA_a [Homo sapiens]	N/A	31
gi|189030	nonmuscle myosin heavy chain-A	82322	31
gi|18916806	KIAA1962 protein [Homo sapiens]	87198	30
gi|2392338	Chain A, Human Glyoxalase I With Benzyl-Glutathione Inhibitor	20861	198
gi|3891517	Chain A, Human Glyoxalase I Q33e, E172q Double Mutant	20861	75
gi|34740335	tubulin, alpha 1B [Mus musculus]	50804	408
gi|37492	alpha-tubulin [Homo sapiens]	50810	34
gi|158259731	unnamed protein product [Homo sapiens]	50788	364
gi|2843123	alpha tubulin [Homo sapiens]	50481	258
gi|32015	alpha-tubulin [Homo sapiens]	50503	204
gi|7106439	tubulin, beta 5 [Mus musculus]	50095	182
gi|9507215	tubulin, alpha 8 [Homo sapiens]	50746	145
gi|31873439	hypothetical protein [Homo sapiens]	54619	145
gi|5174735	tubulin, beta, 2 [Homo sapiens]	50255	138
gi|27754056	tubulin, beta 6 [Mus musculus]	50514	122
gi|30582781	tubulin, beta, 4 [Homo sapiens]	89693	121
gi|89574029	mitochondrial ATP synthase, H+ transporting F1 complex beta subunit [Homo sapiens]	48083	107
gi|28940	unnamed protein product [Homo sapiens]	57976	107
gi|28317	unnamed protein product [Homo sapiens]	59720	128
gi|4501885	beta actin [Homo sapiens]	42052	86
gi|119587277	hCG19802, isoform CRA_b [Homo sapiens]	41841	82
gi|62896585	adenylyl cyclase-associated protein variant [Homo sapiens]	51899	62
gi|134133226	protein expressed in prostate, ovary, testis, and placenta 2 [Homo sapiens]	122882	80
gi|4501881	alpha 1 actin precursor [Homo sapiens]	42366	73
gi|113413200	PREDICTED: similar to protein expressed in prostate, ovary, testis, and placenta 2 [Homo sapiens]	118740	71
gi|169162260	PREDICTED: similar to hornerin [Homo sapiens]	191082	64
gi|1710248	protein disulfide isomerase-related protein 5 [Homo sapiens]	46512	64
gi|35959	tubulin 5-beta [Homo sapiens]	50055	62
gi|119625004	tubulin, beta polypeptide 4, member Q [Homo sapiens]	50698	52
gi|1857526	beta-tubulin [Homo sapiens]	48860	52
gi|223486	tubulin beta	49830	50
gi|169167253	PREDICTED: similar to tubulin, beta polypeptide 4, member Q [Homo sapiens]	51277	48
gi|21749301	unnamed protein product [Homo sapiens]	21359	46
gi|13562114	beta tubulin 1, class VI [Homo sapiens]	50865	45

gi|10433717	unnamed protein product [Homo sapiens]	50267	45
gi|113423449	PREDICTED: similar to hCG1791842 isoform 1 [Homo sapiens]	56600	43
gi|703118	thyroid receptor interactor	35892	35
gi|74739412	Kappa-actin	42331	41
gi|62420929	actin-like protein [Homo sapiens]	11517	41
gi|62421029	actin-like protein [Homo sapiens]	11601	41
gi|119586206	hCG1814159 [Homo sapiens]	7393	41
gi|55960095	dystonin [Homo sapiens]	861913	34
gi|34577047	dystonin isoform 1 [Homo sapiens]	632532	34
gi|553734	putative [Homo sapiens]	2269	69
gi|21361091	ubiquitin carboxyl-terminal esterase L1 [Homo sapiens]	25151	40
gi|6808064	hypothetical protein [Homo sapiens]	119391	39
gi|5616074	prostate derived STE20-like kinase PSK [Homo sapiens]	138945	39
gi|7012700	immunoglobulin heavy chain variable region [Homo sapiens]	14134	38
gi|35655	unnamed protein product [Homo sapiens]	57458	38
gi|4506221	proteasome 26S non-ATPase subunit 12 [Homo sapiens]	53270	36
gi|119590696	membrane protein, palmitoylated 4 (MAGUK p55 subfamily member 4), isoform CRA_f [Homo sapiens]	51236	34
gi|119589109	hCG1992890, isoform CRA_b [Homo sapiens]	37492	36
gi|153792148	threonine synthase-like 1 [Homo sapiens]	N/A	36
gi|134254710	tubulin beta 2C [Homo sapiens]	10100	35
gi|89036703	PREDICTED: similar to tubulin, beta 5 [Homo sapiens]	12210	35
gi|119587055	hCG1983510, isoform CRA_a [Homo sapiens]	28083	35
gi|162416245	HEAT repeat-containing protein 5A	N/A	35
gi|55957939	cytoplasmic polyadenylation element binding protein 3 [Homo sapiens]	75021	35
gi|22209060	Cytoplasmic polyadenylation element binding protein 3 [Homo sapiens]	76522	35
gi|113414234	PREDICTED: hypothetical protein [Homo sapiens]	22772	34
gi|312812	propionyl-CoA carboxylase [Homo sapiens]	58796	34
gi|10441899	unknown [Homo sapiens]	33312	34
gi|5822326	Chain A, Human Mitochondrial Nad(P)-Dependent Malic Enzyme	65748	34
gi|93102389	KIAA1712 [Homo sapiens]	44625	34
gi|4759254	TNF receptor-associated factor 6 [Homo sapiens]	61244	34
gi|20987288	GLE1 RNA export mediator homolog (yeast) [Homo sapiens]	N/A	34
gi|23097308	spectrin repeat containing, nuclear envelope 1 isoform 2 [Homo sapiens]	1011226	34
gi|27884034	HZGJ [Homo sapiens]	N/A	34
gi|52630837	immunoglobulin heavy chain variable region [Homo sapiens]	10598	34

gi|115583679	CCR4-NOT transcription complex, subunit 6-like [Homo sapiens]	63474	33
gi|119720	Coagulation factor XIII A chain precursor (Coagulation factor XIIIa) (Protein-glutamine gamma-glutamyltransferase A chain) (Transglutaminase A chain)	N/A	33
gi|113413444	PREDICTED: hypothetical protein [Homo sapiens]	22799	33
gi|4689262	sorting nexin 11 [Homo sapiens]	N/A	33
gi|119607690	hCG1642689, isoform CRA_a [Homo sapiens]	N/A	33
gi|17511753	PH-4 protein [Homo sapiens]	19870	32
gi|2246416	methyl-CpG-binding protein 2 [Homo sapiens]	52508	32
gi|23451218	testis spermatogenesis apoptosis-related protein 3 [Homo sapiens]	17100	32
gi|187240	leukocyte surface protein	83310	31
gi|34226	laminin A chain [Homo sapiens]	297083	30
gi|28606	unnamed protein product [Homo sapiens]	56582	30
gi|41147168	PREDICTED: similar to hCG1989915 [Homo sapiens]	22112	30
gi|28336	mutant beta-actin (beta'-actin) [Homo sapiens]	42128	1183
gi|16359158	Actin, beta [Homo sapiens]	42078	80
gi|4501881	alpha 1 actin precursor [Homo sapiens]	42366	73
gi|4885049	cardiac muscle alpha actin 1 proprotein [Homo sapiens]	42334	791
gi|158254664	unnamed protein product [Homo sapiens]	42362	780
gi|119612724	actin, alpha, cardiac muscle, isoform CRA_c [Homo sapiens]	30498	774
gi|4501889	actin, gamma 2 propeptide [Homo sapiens]	42249	764
gi|153791352	prostate, ovary, testis expressed protein on chromosome 2 [Homo sapiens]	123020	684
gi|119607748	hCG15971, isoform CRA_b [Homo sapiens]	13907	673
gi|134133226	protein expressed in prostate, ovary, testis, and placenta 2 [Homo sapiens]	122882	80
gi|55957587	actin, alpha 2, smooth muscle, aorta [Homo sapiens]	16919	437
gi|74739412	Kappa-actin	42331	41
gi|63055057	actin, beta-like 2 [Homo sapiens]	42318	360
gi|88953571	PREDICTED: similar to protein expressed in prostate, ovary, testis, and placenta 2 isoform 2 [Homo sapiens]	122858	343
gi|62421140	actin-like protein [Homo sapiens]	11861	274
gi|62421128	actin-like protein [Homo sapiens]	11479	267
gi|62420995	actin-like protein [Homo sapiens]	11481	246
gi|2392338	Chain A, Human Glyoxalase I With Benzyl-Glutathione Inhibitor	20861	198
gi|169213772	PREDICTED: similar to actin alpha 1 skeletal muscle protein [Homo sapiens]	51513	139
gi|169161796	PREDICTED: similar to Hornerin [Homo sapiens]	190911	66
gi|62421091	actin-like protein [Homo sapiens]	11509	59
gi|62421089	actin-like protein [Homo sapiens]	11524	59
gi|62420963	actin-like protein [Homo sapiens]	11546	59

gi|62421075	actin-like protein [Homo sapiens]	11519	59
gi|62420949	actin-like protein [Homo sapiens]	11568	58
gi|114147469	immunoglobulin heavy chain variable region [Homo sapiens]	12608	52
gi|88942898	PREDICTED: similar to beta-actin [Homo sapiens]	17467	48
gi|7023699	unnamed protein product [Homo sapiens]	39666	47
gi|10433974	unnamed protein product [Homo sapiens]	114263	47
gi|5031753	heterogeneous nuclear ribonucleoprotein H1 [Homo sapiens]	49484	42
gi|55962124	interleukin enhancer binding factor 2, 45kDa [Homo sapiens]	12375	41
gi|30025501	KIF27B [Homo sapiens]	153360	40
gi|12751452	PDZ domain-containing protein AIPC [Homo sapiens]	N/A	39
gi|6754020	guanine nucleotide binding protein (G protein), gamma 2 subunit [Mus musculus]	7959	38
gi|158261511	unnamed protein product [Homo sapiens]	49828	38
gi|119627366	coiled-coil domain containing 17, isoform CRA_a [Homo sapiens]	62148	38
gi|22761216	unnamed protein product [Homo sapiens]	69927	37
gi|21749301	unnamed protein product [Homo sapiens]	21359	46
gi|56405460	citron [Homo sapiens]	238511	37
gi|34526448	unnamed protein product [Homo sapiens]	53733	46
gi|71891729	KIAA1503 protein [Homo sapiens]	514649	35
gi|62421077	actin-like protein [Homo sapiens]	11603	35
gi|111306451	Heterogeneous nuclear ribonucleoprotein A1 [Homo sapiens]	34245	35
gi|16751921	dermcidin preproprotein [Homo sapiens]	11391	56
gi|19421557	chromodomain helicase DNA binding protein 5 [Homo sapiens]	307754	35
gi|24415828	RIGB [Homo sapiens]	N/A	35
gi|169213053	PREDICTED: hypothetical LOC100131655 [Homo sapiens]	169808	34
gi|10946096	immunoglobulin lambda light chain variable region [Homo sapiens]	9192	34
gi|34534054	unnamed protein product [Homo sapiens]	23821	34
gi|119574495	hCG1990709 [Homo sapiens]	19954	34
gi|39753961	IQ motif containing GTPase activating protein 3 [Homo sapiens]	185169	34
gi|34527841	unnamed protein product [Homo sapiens]	117393	34
gi|119624933	hCG1797215 [Homo sapiens]	10756	34
gi|188684	modulator recognition factor I	66591	33
gi|729833	Interleukin-6 receptor subunit beta precursor (IL-6R-beta) (Interleukin-6 signal transducer) (Membrane glycoprotein 130) (gp130) (Oncostatin-M receptor alpha subunit) (CD130 antigen) (CDw130)	104484	33
gi|553734	putative [Homo sapiens]	2269	69

gi|16553829	unnamed protein product [Homo sapiens]	N/A	33
gi|34039	unnamed protein product [Homo sapiens]	44079	33
gi|5802182	PPAR gamma coactivator-1 [Homo sapiens]	92141	32
gi|16579885	ribosomal protein L4 [Homo sapiens]	47953	32
gi|1841430	heavy neurofilament subunit [Homo sapiens]	111941	32
gi|2661079	similar to beta tubulin [Homo sapiens]	38945	32
gi|30582781	tubulin, beta, 4 [Homo sapiens]	89693	121
gi|18088719	Tubulin, beta [Homo sapiens]	50096	32
gi|223429	tubulin beta	50223	32
gi|119568443	A kinase (PRKA) anchor protein 7, isoform CRA_b [Homo sapiens]	37234	31
gi|7106802	HSPC206 [Homo sapiens]	N/A	31
gi|14017783	KIAA1783 protein [Homo sapiens]	171295	30
gi|119604338	hCG2042381, isoform CRA_b [Homo sapiens]	19607	30

Appendix 2

GI	Gene	Mass	Score
12667788	myosin, heavy polypeptide 9, non-muscle	227646	76
113412358	PREDICTED: similar to Hornerin	188565	56
24638295	Ubiquitin conjugation factor E4 B	147460	53
113413194	POTE ankyrin domain family member F	123020	633
83699649	heat shock 90kDa protein 1, alpha	98652	319
4503483	eukaryotic translation elongation factor 2	96246	197
15010550	heat shock protein gp96 precursor	90309	51
306891	90kDa heat shock protein	83584	424
67477458	Heat shock protein 75 kDa, mitochondrial	80345	87
62089222	heat shock 70kDa protein 1A variant	78018	62
28590	unnamed protein product	71246	148
35222	heat-shock protein HSP70B	71209	99
5729877	heat shock 70kDa protein 8 isoform 1	71082	273
4504965	L-plastin	70815	101
21759781	Heat shock 70kDa protein 1-like	70748	62
188488	heat shock-induced protein	70294	99
4204880	heat shock protein	70237	118
4505257	moesin	67892	106
189238	neuroleukin	63377	77
5453607	chaperonin containing TCP1, subunit 7 isoform a	59842	92
61104915	heat shock protein 90Bd	58855	78
4502643	chaperonin containing TCP1, subunit 6A isoform a	58444	51
35505	pyruvate kinase	58411	433
1200184	stimulator of TAR RNA binding	58316	82
1002923	coronin-like protein	51722	75
9507215	tubulin alpha-8 chain isoform 1	50746	351
14389309	tubulin alpha-1C chain	50548	874
4503471	eukaryotic translation elongation factor 1 alpha 1	50451	234
4507729	tubulin, beta 2	50274	91
223486	tubulin beta	49830	91
34536332	unnamed protein product	49533	57
61104911	heat shock protein 90Bb	49377	105
28557150	hornerin	48797	68
57209813	tubulin, beta polypeptide	48135	134
5803011	enolase 2	47581	330
4503571	alpha-enolase	47481	998
62896593	enolase 1 variant	47453	998
4503573	enolase 3	47271	464

89037243	PREDICTED: similar to actin-like protein	46576	312
12803339	SERPINE1 mRNA binding protein 1	44291	111
927065	eukaryotic translation elongation factor 1 alpha 1-like 14	43139	204
28422655	ENO1P protein	42657	71
4501881	actin, alpha skeletal muscle	42366	1133
62990121	actin-like protein	42331	399
63055057	beta-actin-like protein 2	42318	549
4501885	actin, cytoplasmic 1	42052	1608
10437873	unnamed protein product	41929	209
47078295	adenosine deaminase	41024	55
224877	deaminase a,adenosine	41009	55
5729953	nuclear distribution gene C homolog	38276	59
2521981	alpha2-HS glycoprotein	36268	99
181914	DNA-binding protein	36086	59
10436240	unnamed protein product	27757	149
178045	gamma-actin	26147	774
62420949	actin-like protein	11568	84
62421162	actin-like protein	11529	94
16751921	dermcidin preproprotein	11391	76

References

1. Breslow, R.; Baldwin, S.; Flechtner, T.; Kalicky, P.; Liu, S.; Washburn, W. Remote oxidation of steroids by photolysis of attached benzophenone groups. *J Am Chem Soc* **1973,** 95, 3251-62.

2. Prestwich, G. D.; Dorman, G.; Elliott, J. T.; Marecak, D. M.; Chaudhary, A. Benzophenone photoprobes for phosphoinositides, peptides and drugs. *Photochem Photobiol* **1997,** 65, 222-34.

3. Dorman, G.; Prestwich, G. D. Using photolabile ligands in drug discovery and development. *Trends Biotechnol* **2000,** 18, 64-77.

4. Williams, N.; Ackerman, S. H.; Coleman, P. S. Benzophenone-ATP: a photoaffinity label for the active site of ATPases. *Methods Enzymol* **1986,** 126, 667-82.

5. Aloise, P.; Kagawa, Y.; Coleman, P. S. Comparative Mg(2+)-dependent sequential covalent binding stoichiometries of 3'-O-(4-benzoyl)benzoyl adenosine 5'-diphosphate of MF1, TF1, and the alpha 3 beta 3 core complex of TF1. The binding change motif is independent of the F1 gamma delta epsilon subunits. *J Biol Chem* **1991,** 266, 10368-76.

6. Musier, K. M.; Hammes, G. G. Rotation of nucleotide sites is not required for the enzymatic activity of chloroplast coupling factor 1. *Biochemistry* **1987,** 26, 5982-8.

7. Pal, P. K.; Coleman, P. S. Detecting precatalytic conformational changes in F1-ATPase with 4-benzoyl(benzoyl)-1-amidofluorescein, a novel fluorescent nucleotide site-specific photoaffinity label. *J Biol Chem* **1990,** 265, 14996-5002.

8. Erb, L.; Lustig, K. D.; Ahmed, A. H.; Gonzalez, F. A.; Weisman, G. A. Covalent incorporation of 3'-O-(4-benzoyl)benzoyl-ATP into a P2 purinoceptor in transformed mouse fibroblasts. *J Biol Chem* **1990,** 265, 7424-31.

9. Zarka, A.; Shoshan-Barmatz, V. Characterization and photoaffinity labeling of the ATP binding site of the ryanodine receptor from skeletal muscle. *Eur J Biochem* **1993,** 213, 147-54.

10. Abeijon, C.; Capasso, J. M.; Tal, D.; Vann, W. F.; Hirschberg, C. B. 3'-O-(4-benzoyl)benzoylcytidine 5'-triphosphate. A substrate and photoaffinity label for CMP-N-acetylneuraminic acid synthetase. *J Biol Chem* **1986,** 261, 11374-7.

11. Thalmann, E.; Blaas, D. Synthesis of gamma-[4-(benzoylphenyl)methylamido]-7-methylguanosine 5'-triphosphate, a photoaffinity-label for cap-binding proteins. *Biochim Biophys Acta* **1991,** 1088, 301-4.

12. Chavan, A. J.; Rychlik, W.; Blaas, D.; Kuechler, E.; Watt, D. S.; Rhoads, R. E. Phenyl azide substituted and benzophenone-substituted phosphonamides of 7-methylguanosine 5'-triphosphate as photoaffinity probes for protein synthesis initiation factor eIF-4E and a proteolytic fragment containing the cap-binding site. *Biochemistry* **1990,** 29, 5521-9.

13. Salvucci, M. E.; Rajagopalan, K.; Sievert, G.; Haley, B. E.; Watt, D. S. Photoaffinity labeling of ribulose-1,5-bisphosphate carboxylase/oxygenase activase with ATP gamma-benzophenone. Identification of the ATP gamma-phosphate binding domain. *J Biol Chem* **1993,** 268, 14239-44.

14. Rajagopalan, K.; Chavan, A. J.; Haley, B. E.; Watt, D. S. Synthesis and application of bidentate photoaffinity cross-linking reagents. Nucleotide photoaffinity probes with two photoactive groups. *J Biol Chem* **1993,** 268, 14230-8.

15. Cremo, C. R.; Yount, R. G. 2'-Deoxy-3'-O-(4-benzoylbenzoyl)- and 3'(2')-O-(4-benzoylbenzoyl)-1,N6-ethenoadenosine 5'-diphosphate, fluorescent photoaffinity analogues of adenosine 5'-diphosphate. Synthesis, characterization, and interaction with myosin subfragment 1. *Biochemistry* **1987,** 26, 7524-34.

16. Mahmood, R.; Elzinga, M.; Yount, R. G. Serine-324 of myosin's heavy chain is photoaffinity-labeled by 3'(2')-O-(4-benzoylbenzoyl)adenosine triphosphate. *Biochemistry* **1989,** 28, 3989-95.

17. Ishidate, K.; Matsuo, R.; Nakazawa, Y. CDP-choline: 1,2-diacylglycerol cholinephosphotransferase from rat liver microsomes. II. Photoaffinity labeling by radioactive CDP-choline analogs. *Biochim Biophys Acta* **1992,** 1124, 36-44.

18. Cole, D. G.; Yount, R. G. Photolabeling of the 6 and 10 S conformations of gizzard myosin with 3'(2')-O-(4-Benzoyl)benzoyl-ATP. Proline 324 is near the active site. *J Biol Chem* **1990,** 265, 22537-46.

19. Page, M. G.; Rosenbusch, J. P. Topographic labelling of pore-forming proteins from the outer membrane of Escherichia coli. *Biochem J* **1986,** 235, 651-61.

20. Montecucco, C.; Schiavo, G. 1-Palmitoyl-2-(p-benzoyl)benzoyl phosphatidylcholine, a photoactive phospholipid for the labelling of membrane components. *Biochem J* **1986,** 237, 309-12.

21. Son, C. D.; Sargsyan, H.; Naider, F.; Becker, J. M. Identification of ligand binding regions of the Saccharomyces cerevisiae alpha-factor pheromone receptor by photoaffinity cross-linking. *Biochemistry* **2004,** 43, 13193-203.

22. Henry, L. K.; Khare, S.; Son, C.; Babu, V. V.; Naider, F.; Becker, J. M. Identification of a contact region between the tridecapeptide alpha-factor mating pheromone of Saccharomyces cerevisiae and its G protein-coupled receptor by photoaffinity labeling. *Biochemistry* **2002,** 41, 6128-39.

23. Lee, B. K.; Lee, Y. H.; Hauser, M.; Son, C. D.; Khare, S.; Naider, F.; Becker, J. M. Tyr266 in the sixth transmembrane domain of the yeast alpha-factor receptor plays key roles in receptor activation and ligand specificity. *Biochemistry* **2002,** 41, 13681-9.

24. Miller, W. T. Peptide-based affinity labeling of adenosine cyclic monophosphate-dependent protein kinase. *Methods Enzymol* **1991,** 200, 500-8.

25. Saghatelian, A.; Jessani, N.; Joseph, A.; Humphrey, M.; Cravatt, B. F. Activity-based probes for the proteomic profiling of metalloproteases. *Proc Natl Acad Sci U S A* **2004,** 101, 10000-5.

26. Overall, C. M.; Lopez-Otin, C. Strategies for MMP inhibition in cancer: innovations for the post-trial era. *Nat Rev Cancer* **2002,** 2, 657-72.

27. Chang, C.; Werb, Z. The many faces of metalloproteases: cell growth, invasion, angiogenesis and metastasis. *Trends Cell Biol* **2001,** 11, S37-43.

28. Turner, A. J.; Isaac, R. E.; Coates, D. The neprilysin (NEP) family of zinc metalloendopeptidases: genomics and function. *Bioessays* **2001,** 23, 261-9.

29. Salisbury, C. M.; Cravatt, B. F. Activity-based probes for proteomic profiling of histone deacetylase complexes. *Proc Natl Acad Sci U S A* **2007,** 104, 1171-6.

30. Bolden, J. E.; Peart, M. J.; Johnstone, R. W. Anticancer activities of histone deacetylase inhibitors. *Nat Rev Drug Discov* **2006,** 5, 769-84.

31. Marks, P. A.; Breslow, R. Dimethyl sulfoxide to vorinostat: development of this histone deacetylase inhibitor as an anticancer drug. *Nat Biotechnol* **2007,** 25, 84-90.

32. Kan, T.; Tominari, Y.; Morohashi, Y.; Natsugari, H.; Tomita, T.; Iwatsubo, T.; Fukuyama, T. Solid-phase synthesis of photoaffinity probes: highly efficient

incorporation of biotin-tag and cross-linking groups. *Chem Commun (Camb)* **2003**, 2244-5.

33. Lamos, S. M.; Krusemark, C. J.; McGee, C. J.; Scalf, M.; Smith, L. M.; Belshaw, P. J. Mixed isotope photoaffinity reagents for identification of small-molecule targets by mass spectrometry. *Angew Chem Int Ed Engl* **2006,** 45, 4329-33.

34. Guo, L. W.; Hajipour, A. R.; Gavala, M. L.; Arbabian, M.; Martemyanov, K. A.; Arshavsky, V. Y.; Ruoho, A. E. Sulfhydryl-reactive, cleavable, and radioiodinatable benzophenone photoprobes for study of protein-protein interaction. *Bioconjug Chem* **2005,** 16, 685-93.

35. van Scherpenzeel, M.; van der Pot, M.; Arnusch, C. J.; Liskamp, R. M.; Pieters, R. J. Detection of galectin-3 by novel peptidic photoprobes. *Bioorg Med Chem Lett* **2007,** 17, 376-8.

36. Kato, E.; Howitt, R.; Dzyuba, S. V.; Nakanishi, K. Synthesis of novel ginkgolide photoaffinity--biotin probes. *Org Biomol Chem* **2007,** 5, 3758-61.

37. Yamazaki, Y.; Kohno, K.; Yasui, H.; Kiso, Y.; Akamatsu, M.; Nicholson, B.; Deyanat-Yazdi, G.; Neuteboom, S.; Potts, B.; Lloyd, G. K.; Hayashi, Y. Tubulin photoaffinity labeling with biotin-tagged derivatives of potent diketopiperazine antimicrotubule agents. *Chembiochem* **2008,** 9, 3074-81.

38. Nunes, M.; Kaplan, J.; Wooters, J.; Hari, M.; Minnick, A. A., Jr.; May, M. K.; Shi, C.; Musto, S.; Beyer, C.; Krishnamurthy, G.; Qiu, Y.; Loganzo, F.; Ayral-Kaloustian, S.; Zask, A.; Greenberger, L. M. Two photoaffinity analogues of the tripeptide, hemiasterlin, exclusively label alpha-tubulin. *Biochemistry* **2005,** 44, 6844-57.

39. van Scherpenzeel, M.; Moret, E. E.; Ballell, L.; Liskamp, R. M.; Nilsson, U. J.; Leffler, H.; Pieters, R. J. Synthesis and evaluation of new thiodigalactoside-based chemical probes to label galectin-3. *Chembiochem* **2009,** 10, 1724-33.

40. Tian, R.; Li, L.; Tang, W.; Liu, H.; Ye, M.; Zhao, Z. K.; Zou, H. Chemical proteomic study of isoprenoid chain interactome with a synthetic photoaffinity probe. *Proteomics* **2008,** 8, 3094-104.

41. Olivo, H. F.; Perez-Hernandez, N.; Liu, D.; Iruthayanathan, M.; O'Leary, B.; Homan, L. L.; Dillon, J. S. Synthesis and application of a photoaffinity analog of dehydroepiandrosterone (DHEA). *Bioorg Med Chem Lett* 20, 1153-5.

42. Ballell, L.; Alink, K. J.; Slijper, M.; Versluis, C.; Liskamp, R. M.; Pieters, R. J. A new chemical probe for proteomics of carbohydrate-binding proteins. *Chembiochem* **2005,** 6, 291-5.

43. Chan, E. W.; Chattopadhaya, S.; Panicker, R. C.; Huang, X.; Yao, S. Q. Developing photoactive affinity probes for proteomic profiling: hydroxamate-based probes for metalloproteases. *J Am Chem Soc* **2004,** 126, 14435-46.

44. Sieber, S. A.; Niessen, S.; Hoover, H. S.; Cravatt, B. F. Proteomic profiling of metalloprotease activities with cocktails of active-site probes. *Nat Chem Biol* **2006,** 2, 274-81.

45. Salisbury, C. M.; Cravatt, B. F. Optimization of activity-based probes for proteomic profiling of histone deacetylase complexes. *J Am Chem Soc* **2008,** 130, 2184-94.

46. Chant, I. D.; Rose, P. E.; Morris, A. G. Analysis of heat-shock protein expression in myeloid leukaemia cells by flow cytometry. *Br J Haematol* **1995,** 90, 163-8.

47. Yeh, C.-H.; Tseng, R.; Zhang, Z.; Cortes, J.; O'Brien, S.; Giles, F.; Hannah, A.; Estrov, Z.; Keating, M.; Kantarjian, H.; Albitar, M. Circulating heat shock protein 70 and progression in patients with chronic myeloid leukemia. *Leukemia Research* **2009,** 33, 212-217.

48. Pockley, A. G.; Wu, R.; Lemne, C.; Kiessling, R.; de Faire, U.; Frostegard, J. Circulating heat shock protein 60 is associated with early cardiovascular disease. *Hypertension* **2000,** 36, 303-7.

49. Pockley, A. G.; De Faire, U.; Kiessling, R.; Lemne, C.; Thulin, T.; Frostegard, J. Circulating heat shock protein and heat shock protein antibody levels in established hypertension. *J Hypertens* **2002,** 20, 1815-20.

50. Pockley, A. G.; Georgiades, A.; Thulin, T.; de Faire, U.; Frostegard, J. Serum heat shock protein 70 levels predict the development of atherosclerosis in subjects with established hypertension. *Hypertension* **2003,** 42, 235-8.

51. Adewoye, A. H.; Klings, E. S.; Farber, H. W.; Palaima, E.; Bausero, M. A.; McMahon, L.; Odhiambo, A.; Surinder, S.; Yoder, M.; Steinberg, M. H.; Asea, A. Sickle cell vaso-occlusive crisis induces the release of circulating serum heat shock protein-70. *Am J Hematol* **2005,** 78, 240-2.

52. Wright, B. H.; Corton, J. M.; El-Nahas, A. M.; Wood, R. F.; Pockley, A. G. Elevated levels of circulating heat shock protein 70 (Hsp70) in peripheral and renal vascular disease. *Heart Vessels* **2000,** 15, 18-22.

53. Dorman, G.; Prestwich, G. D. Benzophenone photophores in biochemistry. *Biochemistry* **1994,** 33, 5661-73.

54. Saviano, M.; Improta, R.; Benedetti, E.; Carrozzini, B.; Cascarano, G. L.; Didierjean, C.; Toniolo, C.; Crisma, M. Benzophenone photophore flexibility and proximity: molecular and crystal-state structure of a Bpa-containing trichogin dodecapeptide analogue. *Chembiochem* **2004,** 5, 541-4.

55. Vodovozova, E. L. Photoaffinity labeling and its application in structural biology *Biochemistry (Moscow)* **2007,** 72, 1-16.

56. Kauer, J. C.; Erickson-Viitanen, S.; Wolfe, H. R., Jr.; DeGrado, W. F. p-Benzoyl-L-phenylalanine, a new photoreactive amino acid. Photolabeling of calmodulin with a synthetic calmodulin-binding peptide. *J Biol Chem* **1986,** 261, 10695-700.

57. Dong, M.; Li, Z.; Pinon, D. I.; Lybrand, T. P.; Miller, L. J. Spatial approximation between the amino terminus of a peptide agonist and the top of the sixth transmembrane segment of the secretin receptor. *J Biol Chem* **2004,** 279, 2894-903.

58. Winnik, M. A. Cyclization and the conformation of the hydrocarbon chains. *Chem Rev* **1981,** 81, 491-524.

59. Wagner, P. J. Conformational flexibility and photochemistry *Acc Chem Res* **1983,** 16, 461-467.

60. Wittelsberger, A.; Mierke, D. F.; Rosenblatt, M. Mapping ligand-receptor interfaces: approaching the resolution limit of benzophenone-based photoaffinity scanning. *Chem Biol Drug Des* **2008,** 71, 380-3.

61. Hindi, S.; Deng, H.; James, L.; Kawamura, A. Selective photolabeling of Lck kinase in complex proteome. *Bioorg Med Chem Lett* **2006,** 16, 5625-8.

62. Molina, T. J.; Kishihara, K.; Siderovski, D. P.; van Ewijk, W.; Narendran, A.; Timms, E.; Wakeham, A.; Paige, C. J.; Hartmann, K. U.; Veillette, A.; et al. Profound block in thymocyte development in mice lacking p56lck. *Nature* **1992,** 357, 161-4.

63. Anderson, S. J.; Levin, S. D.; Perlmutter, R. M. Protein tyrosine kinase p56lck controls allelic exclusion of T-cell receptor beta-chain genes. *Nature* **1993,** 365, 552-4.

64. Palacios, E. H.; Weiss, A. Function of the Src-family kinases, Lck and Fyn, in T-cell development and activation. *Oncogene* **2004,** 23, 7990-8000.

65. Goldman, F. D.; Ballas, Z. K.; Schutte, B. C.; Kemp, J.; Hollenback, C.; Noraz, N.; Taylor, N. Defective expression of p56lck in an infant with severe combined immunodeficiency. *J Clin Invest* **1998,** 102, 421-9.

66. Marth, J. D.; Cooper, J. A.; King, C. S.; Ziegler, S. F.; Tinker, D. A.; Overell, R. W.; Krebs, E. G.; Perlmutter, R. M. Neoplastic transformation induced by an activated lymphocyte-specific protein tyrosine kinase (pp56lck). *Mol Cell Biol* **1988,** 8, 540-50.

67. Fields, G. B.; Noble, R. L. Solid phase peptide synthesis utilizing 9-fluorenylmethoxycarbonyl amino acids. *Int J Pept Protein Res* **1990,** 35, 161-214.

68. Kawamura, A.; Hindi, S.; Mihai, D. M.; James, L.; Aminova, O. Binding is not enough: flexibility is needed for photocrosslinking of Lck kinase by benzophenone photoligands. *Bioorg Med Chem* **2008,** 16, 8824-9.

69. DeGraw, A. J.; Zhao, Z.; Strickland, C. L.; Taban, A. H.; Hsieh, J.; Jefferies, M.; Xie, W.; Shintani, D. K.; McMahan, C. M.; Cornish, K.; Distefano, M. D. A photoactive isoprenoid diphosphate analogue containing a stable phosphonate linkage: synthesis and biochemical studies with prenyltransferases. *J Org Chem* **2007,** 72, 4587-95.

70. Qvit, N.; Monderer-Rothkoff, G.; Ido, A.; Shalev, D. E.; Amster-Choder, O.; Gilon, C. Development of bifunctional photoactivatable benzophenone probes and their application to glycoside substrates. *Biopolymers* **2008,** 90, 526-36.

71. Fuwa, H.; Hiromoto, K.; Takahashi, Y.; Yokoshima, S.; Kan, T.; Fukuyama, T.; Iwatsubo, T.; Tomita, T.; Natsugari, H. Synthesis of biotinylated photoaffinity probes based on arylsulfonamide gamma-secretase inhibitors. *Bioorg Med Chem Lett* **2006,** 16, 4184-9.

72. Shen, R.; Inoue, T.; Forgac, M.; Porco, J. A., Jr. Synthesis of photoactivatable acyclic analogues of the lobatamides. *J Org Chem* **2005,** 70, 3686-92.

73. Severance, D.; Pandey, B.; Morrison, H. Reaction Path Analysis of Hydrogen Abstraction by the Formaldehyde Triple State *J Am Chem Soc* **1987,** 109, 3231-3233.

74. Wagner, P. J.; Pabon, R.; Park, B. S.; Zand, A. R.; Ward, D. L. The Regioselectivity of Internal Hydrogen Abstraction by Triplet o-tert-Amylbenzophenone. *J Am Chem Soc* **1994,** 116, 589-596.

75. O'Neil, K. T.; DeGrado, W. F. The interaction of calmodulin with fluorescent and photoreactive model peptides: evidence for a short interdomain separation. *Proteins* **1989,** 6, 284-93.

76. Kaiser, E.; Colescott, R. L.; Bossinger, C. D.; Cook, P. I. Color test for detection of free terminal amino groups in the solid-phase synthesis of peptides. *Anal Biochem* **1970,** 34, 595-8.

77. Kantor, T. G. Ketoprofen: a review of its pharmacologic and clinical properties. *Pharmacotherapy* **1986,** 6, 93-103.

78. Kawamura, A.; Hindi, S. Protein fishing with chiral molecular baits. *Chirality* **2005,** 17, 332-7.

79. Weber, P. C.; Ohlendorf, D. H.; Wendoloski, J. J.; Salemme, F. R. Structural origins of high-affinity biotin binding to streptavidin. *Science* **1989,** 243, 85-8.

80. Green, N. M. Avidin and streptavidin. *Methods Enzymol* **1990,** 184, 51-67.

81. Bayer, E. A.; Wilchek, M. Biotin-binding proteins: overview and prospects. *Methods Enzymol* **1990,** 184, 49-51.

82. Abraham, R. T.; Weiss, A. Jurkat T cells and development of the T-cell receptor signalling paradigm. *Nat Rev Immunol* **2004,** 4, 301-8.

83. Tsuchiya, S.; Yamabe, M.; Yamaguchi, Y.; Kobayashi, Y.; Konno, T.; Tada, K. Establishment and characterization of a human acute monocytic leukemia cell line (THP-1). *Int J Cancer* **1980,** 26, 171-6.

84. Hsu, S. H.; Schacter, B. Z.; Delaney, N. L.; Miller, T. B.; McKusick, V. A.; Kennett, R. H.; Bodmer, J. G.; Young, D.; Bodmer, W. F. Genetic characteristics of the HeLa cell. *Science* **1976,** 191, 392-4.

85. Bubenik, J.; Baresova, M.; Viklicky, V.; Jakoubkova, J.; Sainerova, H.; Donner, J. Established cell line of urinary bladder carcinoma (T24) containing tumour-specific antigen. *Int J Cancer* **1973,** 11, 765-73.

86. Soule, H. D.; Vazguez, J.; Long, A.; Albert, S.; Brennan, M. A human cell line from a pleural effusion derived from a breast carcinoma. *J Natl Cancer Inst* **1973,** 51, 1409-16.

87. Wan, H.; Dawson, M. I.; Hong, W. K.; Lotan, R. Enhancement of Calu-1 human lung carcinoma cell growth in serum-free medium by retinoids: dependence on AP-1 activation, but not on retinoid response element activation. *Oncogene* **1997,** 15, 2109-18.

88. Steen, H.; Mann, M. The ABC's (and XYZ's) of peptide sequencing. *Mol Cell Biol* **2004,** 5, 699-711.

89. Thornalley, P. J. The glyoxalase system in health and disease. *Mol Aspects Med* **1993,** 14, 287-371.

90. Creighton, D. J.; Zheng, Z. B.; Holewinski, R.; Hamilton, D. S.; Eiseman, J. L. Glyoxalase I inhibitors in cancer chemotherapy. *Biochem Soc Trans* **2003,** 31, 1378-82.

91. Sakamoto, H.; Mashima, T.; Sato, S.; Hashimoto, Y.; Yamori, T.; Tsuruo, T. Selective activation of apoptosis program by S-p-bromobenzylglutathione cyclopentyl diester in glyoxalase I-overexpressing human lung cancer cells. *Clin Cancer Res* **2001,** 7, 2513-8.

92. Thornalley, P. J. Glyoxalase I--structure, function and a critical role in the enzymatic defence against glycation. *Biochem Soc Trans* **2003,** 31, 1343-8.

93. Thornalley, P. J. Glutathione-dependent detoxification of alpha-oxoaldehydes by the glyoxalase system: involvement in disease mechanisms and antiproliferative activity of glyoxalase I inhibitors. *Chem Biol Interact* **1998,** 111-112, 137-51.

94. Chen, F.; Wollmer, M. A.; Hoerndli, F.; Munch, G.; Kuhla, B.; Rogaev, E. I.; Tsolaki, M.; Papassotiropoulos, A.; Gotz, J. Role for glyoxalase I in Alzheimer's disease. *Proc Natl Acad Sci U S A* **2004,** 101, 7687-92.

95. Santel, T.; Pflug, G.; Hemdan, N. Y.; Schafer, A.; Hollenbach, M.; Buchold, M.; Hintersdorf, A.; Lindner, I.; Otto, A.; Bigl, M.; Oerlecke, I.; Hutschenreuter, A.; Sack, U.; Huse, K.; Groth, M.; Birkemeyer, C.; Schellenberger, W.; Gebhardt, R.; Platzer, M.; Weiss, T.; Vijayalakshmi, M. A.; Kruger, M.; Birkenmeier, G.

Curcumin inhibits glyoxalase 1: a possible link to its anti-inflammatory and anti-tumor activity. *PLoS One* **2008,** 3, e3508.

96. Takasawa, R.; Takahashi, S.; Saeki, K.; Sunaga, S.; Yoshimori, A.; Tanuma, S. Structure-activity relationship of human GLO I inhibitory natural flavonoids and their growth inhibitory effects. *Bioorg Med Chem* **2008,** 16, 3969-75.

97. More, S. S.; Vince, R. Inhibition of glyoxalase I: the first low-nanomolar tight-binding inhibitors. *J Med Chem* **2009,** 52, 4650-6.

98. Thornalley, P. J.; Strath, M.; Wilson, R. J. Antimalarial activity in vitro of the glyoxalase I inhibitor diester, S-p-bromobenzylglutathione diethyl ester. *Biochem Pharmacol* **1994,** 47, 418-20.

99. Chen X., W. S., Wu N., Yang C.S. Leukotriene A4 hydrolase as a target for cancer prevention and therapy *Current Cancer Drug Targets* **2004,** 4, 267-283.

100. Haeggstrom, J. Z. Structure, function, and regulation of leukotriene A4 hydrolase. *Am J Respir Crit Care Med* **2000,** 161, S25-31.

101. Haeggstrom, J. Z.; Kull, F.; Rudberg, P. C.; Tholander, F.; Thunnissen, M. M. Leukotriene A4 hydrolase. *Prostaglandins Other Lipid Mediat* **2002,** 68-69, 495-510.

102. Minami, M.; Ohno, S.; Kawasaki, H.; Radmark, O.; Samuelsson, B.; Jornvall, H.; Shimizu, T.; Seyama, Y.; Suzuki, K. Molecular cloning of a cDNA coding for human leukotriene A4 hydrolase. Complete primary structure of an enzyme involved in eicosanoid synthesis. *J Biol Chem* **1987,** 262, 13873-6.

103. Rudberg, P. C.; Tholander, F.; Andberg, M.; Thunnissen, M. M.; Haeggstrom, J. Z. Leukotriene A4 hydrolase: identification of a common carboxylate recognition site for the epoxide hydrolase and aminopeptidase substrates. *J Biol Chem* **2004,** 279, 27376-82.

104. Funk, C. D.; Radmark, O.; Fu, J. Y.; Matsumoto, T.; Jornvall, H.; Shimizu, T.; Samuelsson, B. Molecular cloning and amino acid sequence of leukotriene A4 hydrolase. *Proc Natl Acad Sci U S A* **1987,** 84, 6677-81.

105. Mancini, J. A.; Evans, J. F. Cloning and characterization of the human leukotriene A4 hydrolase gene. *Eur J Biochem* **1995,** 231, 65-71.

106. Penning, T. D. Inhibitors of leukotriene A4 (LTA4) hydrolase as potential anti-inflammatory agents. *Curr Pharm Des* **2001,** 7, 163-79.

107. Stelzl, U.; Worm, U.; Lalowski, M.; Haenig, C.; Brembeck, F. H.; Goehler, H.; Stroedicke, M.; Zenkner, M.; Schoenherr, A.; Koeppen, S.; Timm, J.; Mintzlaff, S.; Abraham, C.; Bock, N.; Kietzmann, S.; Goedde, A.; Toksoz, E.; Droege, A.; Krobitsch, S.; Korn, B.; Birchmeier, W.; Lehrach, H.; Wanker, E. E. A human protein-protein interaction network: a resource for annotating the proteome. *Cell* **2005,** 122, 957-68.

108. Hendrick, J. P.; Hartl, F. U. The role of molecular chaperones in protein folding. *FASEB J* **1995,** 9, 1559-69.

109. Hartl, F. U.; Hayer-Hartl, M. Molecular chaperones in the cytosol: from nascent chain to folded protein. *Science* **2002,** 295, 1852-8.

110. Agashe, V. R.; Hartl, F. U. Roles of molecular chaperones in cytoplasmic protein folding. *Semin Cell Dev Biol* **2000,** 11, 15-25.

111. Mayer, M. P.; Bukau, B. Hsp70 chaperones: cellular functions and molecular mechanism. *Cell Mol Life Sci* **2005,** 62, 670-84.

112. Hartl, F. U. Molecular chaperones in cellular protein folding. *Nature* **1996,** 381, 571-9.

113. Flynn, G. C.; Pohl, J.; Flocco, M. T.; Rothman, J. E. Peptide-binding specificity of the molecular chaperone BiP. *Nature* **1991,** 353, 726-30.

114. Beckmann, R. P.; Mizzen, L. E.; Welch, W. J. Interaction of Hsp 70 with newly synthesized proteins: implications for protein folding and assembly. *Science* **1990,** 248, 850-4.

115. Sherman, M.; Multhoff, G. Heat shock proteins in cancer. *Ann N Y Acad Sci* **2007,** 1113, 192-201.

116. Ciocca, D. R.; Calderwood, S. K. Heat shock proteins in cancer: diagnostic, prognostic, predictive, and treatment implications. *Cell Stress Chaperones* **2005,** 10, 86-103.

117. Johnson, J. D.; Fleshner, M. Releasing signals, secretory pathways, and immune function of endogenous extracellular heat shock protein 72. *J Leukoc Biol* **2006,** 79, 425-34.

118. Schmitt, E.; Gehrmann, M.; Brunet, M.; Multhoff, G.; Garrido, C. Intracellular and extracellular functions of heat shock proteins: repercussions in cancer therapy. *J Leukoc Biol* **2007,** 81, 15-27.

119. Lewthwaite, J.; Owen, N.; Coates, A.; Henderson, B.; Steptoe, A. Circulating human heat shock protein 60 in the plasma of British civil servants: relationship to physiological and psychosocial stress. *Circulation* **2002,** 106, 196-201.

120. Pesce, A. J.; Michael, J. G. Artifacts and limitations of enzyme immunoassay. *J Immunol Methods* **1992,** 150, 111-9.

121. Leng, S. X.; McElhaney, J. E.; Walston, J. D.; Xie, D.; Fedarko, N. S.; Kuchel, G. A. ELISA and multiplex technologies for cytokine measurement in inflammation and aging research. *J Gerontol A Biol Sci Med Sci* **2008,** 63, 879-84.

122. Welch, W. J.; Garrels, J. I.; Thomas, G. P.; Lin, J. J.; Feramisco, J. R. Biochemical characterization of the mammalian stress proteins and identification of two stress proteins as glucose- and Ca2+-ionophore-regulated proteins. *J Biol Chem* **1983,** 258, 7102-11.

123. Kelley, P. M.; Schlesinger, M. J. Antibodies to two major chicken heat shock proteins cross-react with similar proteins in widely divergent species. *Mol Cell Biol* **1982,** 2, 267-74.

124. Scroggins, B. T.; Neckers, L. Post-translational modification of heat-shock protein 90: impact on chaperone function *Expert Opin. Drug Discov.* **2007,** 2, 1403-1414.

125. Legagneux, V.; Dubois, M. F.; Morange, M.; Bensaude, O. Phosphorylation of the 90 kDa heat shock protein in heat shocked HeLa cell lysates. *FEBS Lett* **1988,** 231, 417-20.

126. Lees-Miller, S. P.; Anderson, C. W. Two human 90-kDa heat shock proteins are phosphorylated in vivo at conserved serines that are phosphorylated in vitro by casein kinase II. *J Biol Chem* **1989,** 264, 2431-7.

127. Choudhary, C.; Kumar, C.; Gnad, F.; Nielsen, M. L.; Rehman, M.; Walther, T. C.; Olsen, J. V.; Mann, M. Lysine acetylation targets protein complexes and co-regulates major cellular functions. *Science* **2009,** 325, 834-40.

128. Wang, Y.; Wang, S. Y.; Zhang, X. H.; Zhao, M.; Hou, C. M.; Xu, Y. J.; Du, Z. Y.; Yu, X. D. FK228 inhibits Hsp90 chaperone function in K562 cells via hyperacetylation of Hsp70. *Biochem Biophys Res Commun* **2007,** 356, 998-1003.

129. Henrikson, K. P.; Allen, S. H.; Maloy, W. L. An avidin monomer affinity column for the purification of biotin-containing enzymes. *Anal Biochem* **1979,** 94, 366-70.

130. Wu, S. C.; Wong, S. L. Intracellular production of a soluble and functional monomeric streptavidin in Escherichia coli and its application for affinity purification of biotinylated proteins. *Protein Expr Purif* **2006,** 46, 268-73.

131. Bayer, E. A.; Wilchek, M. Application of avidin-biotin technology to affinity-based separations. *J Chromatogr* **1990,** 510, 3-11.

132. Kohanski, R. A.; Lane, M. D. Monovalent avidin affinity columns. *Methods Enzymol* **1990,** 184, 194-200.

133. Laitinen, O. H.; Nordlund, H. R.; Hytonen, V. P.; Uotila, S. T.; Marttila, A. T.; Savolainen, J.; Airenne, K. J.; Livnah, O.; Bayer, E. A.; Wilchek, M.; Kulomaa, M. S. Rational design of an active avidin monomer. *J Biol Chem* **2003,** 278, 4010-4.

134. Qureshi, M. H.; Wong, S. L. Design, production, and characterization of a monomeric streptavidin and its application for affinity purification of biotinylated proteins. *Protein Expr Purif* **2002,** 25, 409-15.

135. Boschetti, E.; Giorgio Righetti, P. Hexapeptide combinatorial ligand libraries: the march for the detection of the low-abundance proteome continues. *Biotechniques* **2008,** 44, 663-5.

136. Switzer, R. C., 3rd; Merril, C. R.; Shifrin, S. A highly sensitive silver stain for detecting proteins and peptides in polyacrylamide gels. *Anal Biochem* **1979,** 98, 231-7.

137. Winkler, C.; Denker, K.; Wortelkamp, S.; Sickmann, A. Silver- and Coomassie-staining protocols: detection limits and compatibility with ESI MS. *Electrophoresis* **2007,** 28, 2095-9.

138. Anderson, N. L.; Anderson, N. G. The human plasma proteome: history, character, and diagnostic prospects. *Mol Cell Proteomics* **2002,** 1, 845-67.

139. Adkins, J. N.; Varnum, S. M.; Auberry, K. J.; Moore, R. J.; Angell, N. H.; Smith, R. D.; Springer, D. L.; Pounds, J. G. Toward a human blood serum proteome: analysis by multidimensional separation coupled with mass spectrometry. *Mol Cell Proteomics* **2002,** 1, 947-55.

140. Tirumalai, R. S.; Chan, K. C.; Prieto, D. A.; Issaq, H. J.; Conrads, T. P.; Veenstra, T. D. Characterization of the Low Molecular Weight Human Serum Proteome. *Mol Cell Proteomics* **2003,** 2, 1096-1103.

141. Urbas, L.; Brne, P.; Gabor, B.; Barut, M.; Strlic, M.; Petric, T. C.; Strancar, A. Depletion of high-abundance proteins from human plasma using a combination of an affinity and pseudo-affinity column. *Journal of Chromatography A* **2009,** 1216, 2689-2694.

142. Righetti, P. G.; Boschetti, E.; Lomas, L.; Citterio, A. Protein Equalizer Technology : the quest for a "democratic proteome". *Proteomics* **2006,** 6, 3980-92.

143. Boschetti, E.; Righetti, P. G. The art of observing rare protein species in proteomes with peptide ligand libraries. *Proteomics* **2009,** 9, 1492-510.

144. Sennels, L.; Salek, M.; Lomas, L.; Boschetti, E.; Righetti, P. G.; Rappsilber, J. Proteomic analysis of human blood serum using peptide library beads. *J Proteome Res* **2007,** 6, 4055-62.

145. Shores, K. S.; Udugamasooriya, D. G.; Kodadek, T.; Knapp, D. R. Use of peptide analogue diversity library beads for increased depth of proteomic analysis: application to cerebrospinal fluid. *J Proteome Res* **2008,** 7, 1922-31.

146. Alluri, P. G.; Reddy, M. M.; Bachhawat-Sikder, K.; Olivos, H. J.; Kodadek, T. Isolation of protein ligands from large peptoid libraries. *J Am Chem Soc* **2003,** 125, 13995-4004.

147. Alluri, P.; Liu, B.; Yu, P.; Xiao, X.; Kodadek, T. Isolation and characterization of coactivator-binding peptoids from a combinatorial library. *Mol Biosyst* **2006,** 2, 568-79.

148. Lim, H. S.; Reddy, M. M.; Xiao, X.; Wilson, J.; Wilson, R.; Connell, S.; Kodadek, T. Rapid identification of improved protein ligands using peptoid microarrays. *Bioorg Med Chem Lett* **2009,** 19, 3866-9.

149. Kodadek, T.; Bachhawat-Sikder, K. Optimized protocols for the isolation of specific protein-binding peptides or peptoids from combinatorial libraries displayed on beads. *Mol Biosyst* **2006,** 2, 25-35.

150. Etzioni, R.; Urban, N.; Ramsey, S.; McIntosh, M.; Schwartz, S.; Reid, B.; Radich, J.; Anderson, G.; Hartwell, L. The case for early detection. *Nat Rev Cancer* **2003,** 3, 243-52.

151. Jones, M. B.; Krutzsch, H.; Shu, H.; Zhao, Y.; Liotta, L. A.; Kohn, E. C.; Petricoin, E. F., 3rd. Proteomic analysis and identification of new biomarkers and therapeutic targets for invasive ovarian cancer. *Proteomics* **2002,** 2, 76-84.

152. Petricoin, E. F.; Ardekani, A. M.; Hitt, B. A.; Levine, P. J.; Fusaro, V. A.; Steinberg, S. M.; Mills, G. B.; Simone, C.; Fishman, D. A.; Kohn, E. C.; Liotta, L. A. Use of proteomic patterns in serum to identify ovarian cancer. *Lancet* **2002,** 359, 572-7.

153. Etzioni, R.; Penson, D. F.; Legler, J. M.; di Tommaso, D.; Boer, R.; Gann, P. H.; Feuer, E. J. Overdiagnosis due to prostate-specific antigen screening: lessons from U.S. prostate cancer incidence trends. *J Natl Cancer Inst* **2002,** 94, 981-90.